© 2018. Published by The Company of Biologists Ltd | Development (2018) 145, dev165092. doi:10.1242/dev.165092

RESEARCH ARTICLE

Rasip1 controls lymphatic vessel lumen maintenance by regulating endothelial cell junctions

Xiaolei Liu[1], Xiaowu Gu[2], Wanshu Ma[1], Michael Oxendine[1], Hyea Jin Gil[1], George E. Davis[3], Ondine Cleaver[2] and Guillermo Oliver[1,*]

ABSTRACT

Although major progress in our understanding of the genes and mechanisms that regulate lymphatic vasculature development has been made, we still do not know how lumen formation and maintenance occurs. Here, we identify the Ras-interacting protein Rasip1 as a key player in this process. We show that lymphatic endothelial cell-specific *Rasip1*-deficient mouse embryos exhibit enlarged and blood-filled lymphatics at embryonic day 14.5. These vessels have patent lumens with disorganized junctions. Later on, as those vessels become fragmented and lumens collapse, cell junctions become irregular. In addition, *Rasip1* deletion at later stages impairs lymphatic valve formation. We determined that *Rasip1* is essential for lymphatic lumen maintenance during embryonic development by regulating junction integrity, as *Rasip1* loss results in reduced levels of junction molecules and defective cytoskeleton organization *in vitro* and *in vivo*. We determined that Rasip1 regulates Cdc42 activity, as deletion of *Cdc42* results in similar phenotypes to those seen following the loss of *Rasip1*. Furthermore, ectopic *Cdc42* expression rescues the phenotypes in *Rasip1*-deficient lymphatic endothelial cells, supporting the suggestion that Rasip1 regulates Cdc42 activity to regulate cell junctions and cytoskeleton organization, which are both activities required for lymphatic lumen maintenance.

KEY WORDS: *Rasip1*, Lymphatic endothelial cells, Endothelial cell junctions, Lumen maintenance, Lymphatic valves, Mouse

INTRODUCTION

The lymphatic vasculature consists of two morphologically different types of vessels, with distinct functions. Blind-ended initial lymphatics are interconnected by discontinuous button-like junctions. Larger collecting lymphatics transport lymph to lymph nodes, in which immune response occurs, and eventually bring lymph back to the blood circulation at the junction with the subclavian veins (Oliver, 2004). Collecting lymphatics are connected by continuous zipper-like junctions and are covered by a basement membrane and smooth muscle cells. They also contain lymphatic valves to prevent lymph backflow. As part of the circulatory system, the lymphatic vasculature is essential for maintaining fluid homeostasis, immune surveillance and fat uptake from the intestinal tract (Schulte-Merker et al., 2011). Malfunction of the lymphatic vasculature leads to congenital or inherited disorders, including lymphedema. The importance of the lymphatic vasculature was not appreciated in full detail until recently, as emerging studies unraveled additional and important functional roles for this vascular network in diseases such as cancer, obesity, atherosclerosis and hypertension (Schulte-Merker et al., 2011; Alitalo, 2011). Recent work also indicates that defects of the lymphatic vasculature could be responsible for some diseases that have not previously been linked to lymphatic malfunction. For example, our previous studies revealed that subtle defects in the lymphatic vasculature (i.e. leakage), leads to obesity in mice heterozygous for the gene encoding the transcription factor Prox1, the activity of which is necessary and sufficient for the specification of lymphatic endothelial cell (LEC) fate (Harvey et al., 2005). Furthermore, recent studies have demonstrated that cardiac lymphatic vessels have repaired heart function in response to cardiac injury (Klotz et al., 2015; Henri et al., 2016). Delivery of vascular endothelial growth factor (VEGF) C stimulates new coronary lymphatic vessel formation, reduces fibrosis and promotes cardiac repair in mice after postcardiac injury (Klotz et al., 2015; Henri et al., 2016; Chen et al., 2016). In addition, two types of recently identified lymphatic vessels, meningeal lymphatics (Louveau et al., 2015) and the Schlemm's canal (Aspelund et al., 2014; Thomson et al., 2014; Kizhatil et al., 2014), are responsible for maintaining fluid homeostasis in the central nervous system and the eye, respectively.

In the last few years, our knowledge about the genes and mechanisms regulating LEC fate specification and lymphatic vasculature development has improved substantially (Yang and Oliver, 2014; Semo et al., 2016; Ma and Oliver, 2017). Crucial for proper lymphatic vasculature function is the presence of a lumen that allows the constant flow of fluids along this vascular network. Surprisingly, we still do not know about the morphological and molecular events that participate in this important process. In the blood vasculature, Ras family members and their regulators are major players in the process of lumen formation (Tan et al., 2008), endothelial cell migration (Tan et al., 2008; Sosnowski et al., 1993), capillary tube assembly (Connolly et al., 2002), blood vessel homeostasis (Komatsu and Ruoslahti, 2005), angiogenesis (Serban et al., 2008; Aitsebaomo et al., 2004) and vascular permeability (Serban et al., 2008). Among the Ras family, Rasip1 is a recently identified Ras-interacting protein characterized as an endomembrane Ras effector (Mitin et al., 2004). In *Xenopus* and in mice, *Rasip1* expression is restricted to endothelial cells (ECs) (Xu et al., 2009). In humans, the most significant single-nucleotide polymorphism associated with defects in retinal venular caliber was identified in the *RASIP1* gene (Ikram et al., 2010). Studies in mouse and zebrafish revealed that *Rasip1* is essential for blood vasculature

[1]Center for Vascular and Developmental Biology, Feinberg Cardiovascular and Renal Research Institute, Feinberg School of Medicine, Northwestern University, Chicago, IL 60611, USA. [2]Department of Molecular Biology, University of Texas Southwestern Medical Center, Dallas, TX 75390, USA. [3]Department of Medical Pharmacology and Physiology, University of Missouri School of Medicine, Columbia, MO 65212, USA.

*Author for correspondence (guillermo.oliver@northwestern.edu)

O.C., 0000-0003-2454-6641; G.O., 0000-0003-3984-7615

Received 28 February 2018; Accepted 11 July 2018

Development (2018) 145, dev165092. doi:10.1242/dev.165092

lumen formation and/or its maintenance (Xu et al., 2011; Wilson et al., 2013; Koo et al., 2016). Functional inactivation of *Rasip1* in mice leads to embryonic lethality at embryonic day (E) 10.5, with homozygous null embryos failing to form obvious lumens in blood vessels (Xu et al., 2011). This same group has also reported that loss of *Rasip1* increases RhoA/ROCK/myosin signaling and dramatically reduces Cdc42/Rac1 signaling (Xu et al., 2011). Rasip1 temporally controls different types of GTPases, which in turn regulate different pools of non-muscle myosin II (NMII) to coordinate junction clearance (remodeling) and actomyosin contractility during vascular tubulogenesis (Barry et al., 2016). As a consequence, *Rasip1*-deficient ECs display defective cell polarity, with mis-localization of junction proteins along the apical/luminal surface, and they fail to adhere to the surrounding extracellular matrix (ECM) (Xu et al., 2011). Thus, according to these reports, Rasip1 acts as an endothelial-specific regulator of GTPase signaling, and controls blood vessel tubulogenesis by regulating EC-EC junctions and integrin-mediated EC-ECM junctions (Xu et al., 2011). However, work by another group argued that blood vessel lumen formation is not affected in *Rasip1*-deficient embryos (Wilson et al., 2013); instead they show that, in these embryos, lumens form but eventually collapse, leading to hemorrhage and embryonic lethality (Wilson et al., 2013), a result suggesting that *Rasip1* activity is instead required for lumen maintenance. Mechanistically, they showed that Rasip1 binds RAP1 to regulate endothelial junction stability (Wilson et al., 2013).

Whether similar players and molecular processes regulate lumen formation and maintenance in lymphatic vessels is not yet known; therefore, we decided to evaluate whether *Rasip1* function could also be required to regulate certain aspects of lymphatic vasculature morphogenesis. We show that LEC-specific *Rasip1* deletion in the mouse leads to embryos with severe edema and dilated lymphatic vessels with defective cell junctions. Initially, mutant lymphatic vessels form lumens; however, later on their lumens collapse, and these vessels become discontinuous and fragmented, and the number of mesenteric lymphatic valves is dramatically reduced. Using cultured LECs, we determined that depletion of *Rasip1* in LECs abolishes *Cdc42* activity, which in turn disrupts LEC junctions, leading to fragmented vessels. Furthermore, we also show that *Cdc42*-deficient embryos largely phenocopy the defective lymphatic junctions and lymphatic valve formation phenotypes observed in *Rasip1*-deficient embryos. These data identify *Rasip1* as a key player in the process of lymphatic vasculature morphogenesis.

RESULTS

Rasip1 is expressed in lymphatic endothelial cells

In the mouse, lymphatic vasculature formation starts at ∼E9.5, when a subpopulation of blood endothelial cells in the cardinal vein (CV) expresses the transcription factor Prox1 (Wigle and Oliver, 1999). These Prox1^{+} lymphatic progenitor cells bud off from the CV and migrate in a dorsal-lateral manner to form lymph sacs, from which, eventually, most of the mammalian lymphatic vasculature will be derived. To determine whether Rasip1 is expressed in LECs, we performed immunostaining at different embryonic stages. As seen in Fig. 1A, at E11.5 Rasip1 is expressed in LEC progenitor cells in the CV and in migrating LECs. At E14.5, Rasip1 expression was detected in Prox1^{+} LECs in the jugular lymph sacs (Fig. 1B) and in dermal lymphatic capillaries (Fig. 1C). At E18.5, mesenteric collecting lymphatics and their valves start to become obvious. Rasip1 expression is detected in those collecting lymphatic vessels and it is highly expressed in the valve-forming cells (Fig. 1D). As has been previously shown for blood endothelial cells (BECs) (Wilson et al., 2013), Rasip1 expression also shows a junctional localization in LECs (Fig. 1C,D). Together, these data identify Rasip1 as a novel endothelial cell marker expressed in both BECs and LECs.

Abnormal lymphatic morphogenesis in LEC-specific *Rasip1*-deficient embryos

Next, we evaluated whether *Rasip1* also has a functional role during lymphatic development. *Rasip1* standard null embryos die at ∼E10 because of impaired blood vessel lumen formation (Xu et al., 2011). Accordingly, to evaluate *Rasip1* lymphatic function, we generated LEC-specific *Rasip1* conditional mutants by crossing *Rasip1*-floxed mice (Xu et al., 2011) with *Lyve1eGFPCre* mice (Pham et al., 2010). Unfortunately, those conditional null embryos (*Lyve1eGFPCre*;*Rasip1*$^{f/f}$) also died at ∼E10, presumably because of yolk sac blood vessel defects, as Lyve1 is expressed in those vessels (Gordon et al., 2008). To overcome this issue, we crossed *Rasip1*$^{f/+}$ mice with *Prox1CreER*^{T2} mice (Srinivasan et al., 2007). Cre activity was induced by tamoxifen (TM) injections at E9.5 and E10.5, and embryos were isolated at E14.5. Initial analysis of *Prox1CreER*^{T2};*Rasip1*$^{f/f}$ (*Rasip1* conditional null) embryos at E14.5 showed that they exhibited severe edema and/or hemorrhage, whereas *Prox1CreER*^{T2};*Rasip*$^{f/+}$ embryos showed no obvious phenotype and were used as controls in all experiments (Fig. S1A). As seen in Fig. S1B-D, *Rasip1* deletion in LECs was very efficient, whereas Rasip1 expression in blood vessels was not affected. Next, the skin of E14.5 *Rasip1* conditional null embryos and control littermates was dissected and the wholemount was stained with antibodies against the blood and lymphatic endothelial cell markers PECAM1, Prox1 and Nrp2 (Fig. 2A-D). Different from the collapsed blood vessel phenotypes that have been reported (Xu et al., 2011; Barry et al., 2015), dermal lymphatic vessels were abnormally dilated in *Rasip1* conditional null embryos (Fig. 2A,B) (PECAM1-stained blood vessels appeared to be normal). As indicated by Ter119 staining, we also observed some blood filled lymphatic vessels in *Rasip1* conditional null embryos at this stage (Fig. 2C,D). To investigate whether a lack of Rasip1 affects lymphatic lumen development, thick vibratome sections of control and *Rasip1* conditional null embryos were collected and stained for Nrp2 and Prox1. Different from Rasip1 function in blood vessels, the lymphatic vessels of E14.5 *Rasip1* conditional null embryos had a lumen that appeared to be abnormally enlarged (Fig. 2E-G). To investigate the possible causes of this phenotype, we analyzed changes in LEC proliferation and apoptosis rates at E14.5. Ki67 immunostaining revealed that the proliferation rate was significantly increased in LECs in *Rasip1* conditional null embryos (Fig. S2A-C). LEC apoptosis, however, showed no differences between control and *Rasip1* conditional nulls (Fig. S2D-F). These data indicate that LEC-specific loss of *Rasip1* increases LEC proliferation, resulting in abnormally dilated lymphatics with enlarged lumens at E14.5.

Defective lymphatic endothelial junctions in LEC-specific *Rasip1*-deficient embryos

Loss of *Rasip1* in blood vessels leads to mis-localization of adhesion junctions during blood vessel tubulogenesis (Xu et al., 2011). Therefore, we evaluated whether similar defects were present in *Rasip1* conditional null embryos. Consistent with previous reports (Yao et al., 2012; Zheng et al., 2014), initial lymphatics exhibit continuous zipper-like junctions in control embryos, as visualized by VE-cadherin (also known as cadherin 5)

Development (2018) 145, dev165092. doi:10.1242/dev.165092

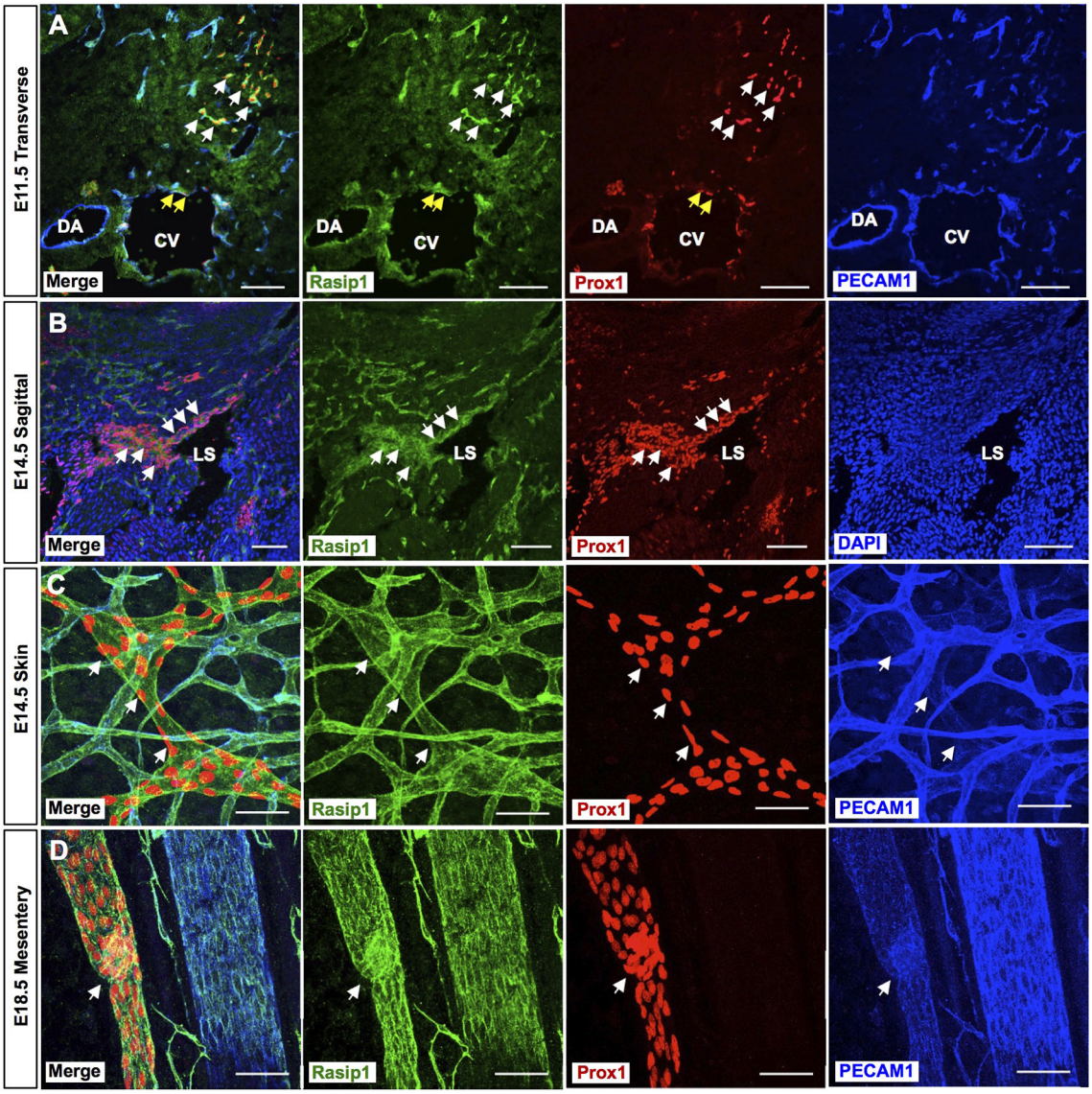

Fig. 1. Rasip1 is expressed in LEC progenitors and lymphatic valve-forming cells. (A) Immunostaining of E11.5 transverse sections. Yellow arrows indicate Rasip1 expression in LEC progenitors in the CV; white arrows indicate Rasip1 expression in initial migrating LECs. *n*=3. DA, dorsal aorta; CV, cardinal vein. (B) Immunostaining of E14.5 sagittal sections. White arrows indicate Rasip1 expression in lymph sacs. *n*=3 embryos. LS, lymph sac. (C) Whole-mount immunostaining of E14.5 dermal lymphatic capillaries. White arrows indicate lymphatic capillaries. *n*=3. (D) Whole-mount immunostaining of E18.5 mesentery collecting lymphatic vessels. Note that Rasip1 expression shows a junctional localization in C and D. *n*=3 embryos. Arrow indicates developing lymphatic valves. Scale bars: 100 µm in A,B; 50 µm in C,D.

immunostaining (Fig. 3A). However, *Rasip1* conditional null embryos exhibited discontinuous and abnormal cell junctions (Fig. 3B). Further characterization showed that tight junctions were also significantly impaired in *Rasip1* conditional null embryos, as revealed by immunofluorescence against ZO-1 (also known as Tjp1) (Fig. 3C,D). This finding was further validated by western blot analysis showing that both VE-cadherin and ZO-1 levels were decreased in dermal LECs, which were isolated from E14.5 *Rasip1* conditional null embryos (Fig. S3A,B). To determine whether this was a general phenotype in developing lymphatics, we analyzed some additional organs and, indeed, similar alterations were also seen, for example, in lung and mesentery-associated lymphatics (Fig. S3C-F).

Because of the severe defects in cell-cell junctions, we next evaluated lymphatic vessel morphogenesis at later stages. At E15.5, dermal lymphatics of *Rasip1* conditional null embryos were still significantly dilated compared with control littermates (Fig. S4). Surprisingly, at ∼E16, these dilated lymphatic vessels in *Rasip1* conditional null embryos still retain a lumen, but start to get fragmented (Fig. 3E,F). Lymphatic endothelial junctions appeared to be discontinued and broken, as revealed by VE-cadherin immunostaining (Fig. 3G,H). Furthermore, lymphatic vessels were narrow and severely disorganized in *Rasip1* conditional null embryos at E16.5 (Fig. 4A,B) and, one day later, those lymphatic vessels appeared to be fragmented and broken (Fig. 4C,D). This phenotype can also be detected in E16.5 collecting lymphatic vessels, in which endothelial cell junctions also appeared to be disorganized (Fig. 4E,F). Eventually, at E17.5 most of the collecting lymphatic vessels were discontinuous and fragmented (Fig. 4G) with narrower lumens and compromised integrity (Fig. 4H,I). These data demonstrated that *Rasip1* is required for proper cell junction organization and, therefore, lymphatic lumen maintenance. To

Development (2018) 145, dev165092. doi:10.1242/dev.165092

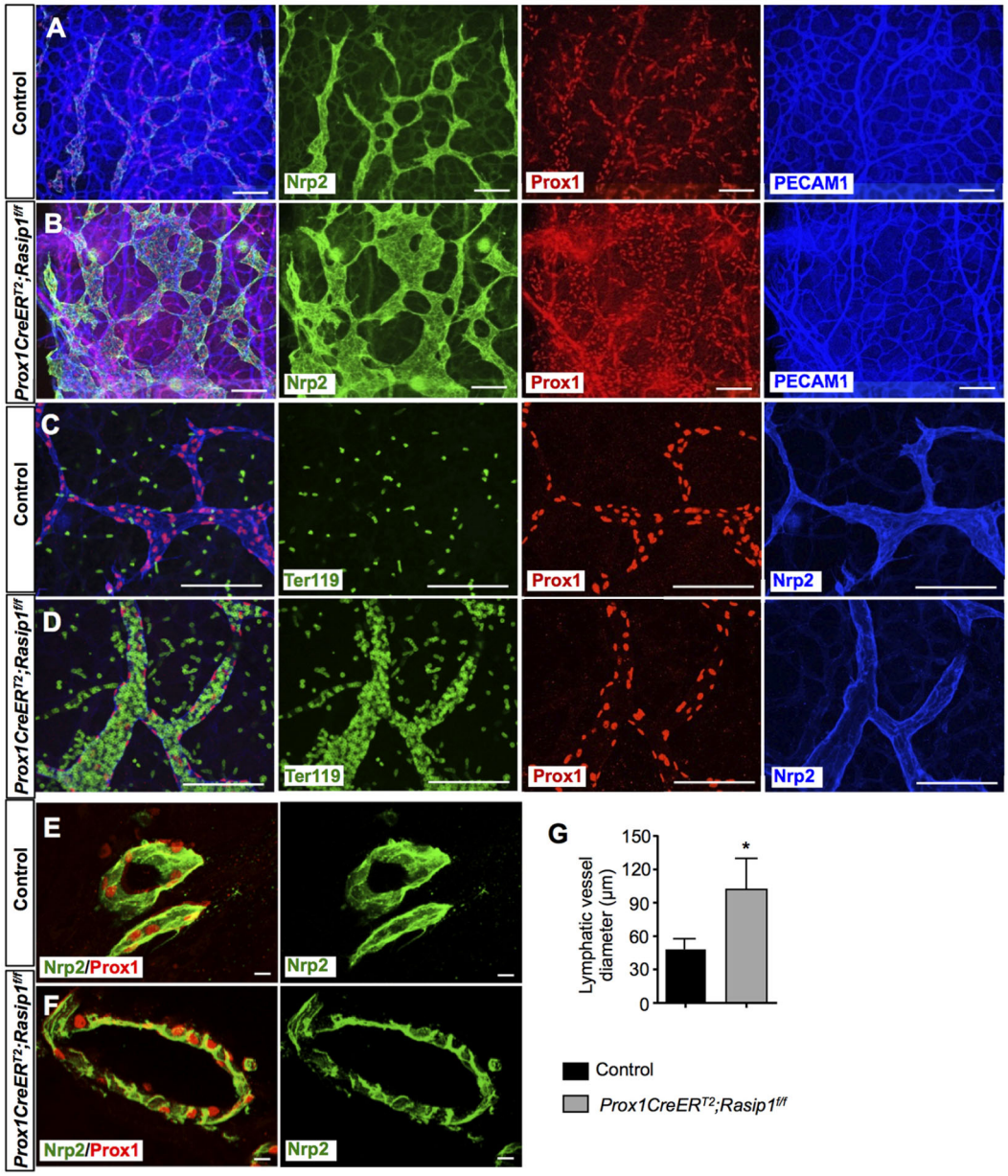

Fig. 2. Enlarged and blood-filled dermal lymphatic capillaries in E14.5 *Prox1CreER^{T2};Rasip1$^{f/f}$* embryos. (A,B) Whole-mount immunostaining of E14.5 control (*n*=3) and *Prox1CreER^{T2};Rasip1$^{f/f}$* (*n*=3) skin showing severely dilated capillary lymphatics in the mutant embryos. (C,D) Whole-mount immunostaining of E14.5 control (*n*=3) and *Prox1CreER^{T2};Rasip1$^{f/f}$* (*n*=3) skin showing blood-filled lymphatics in the mutant embryos. (E,F) Immunostaining of thicker vibratome sections of control (*n*=3) and *Prox1CreER^{T2};Rasip1$^{f/f}$* (*n*=3) embryos showing that lumen formation takes place in *Rasip1* conditional null embryos. However, the diameter of those lumens is enlarged compared with those of control embryos, likely reflecting the enlarged lymphatic capillary. (G) Quantification of lumen diameters in dermal lymphatics of control and *Prox1CreER^{T2};Rasip1$^{f/f}$* embryos. Data are derived from six randomly selected fields per genotype. Data are mean ±s.e.m. **P*<0.05 (Student's *t*-test, versus control). TM was induced at E9.5 and E10.5. Scale bars: 100 µm in A,B; 50 µm in C,D; 25 µm in E,F.

determine whether the broken and collapsed vessel phenotype was associated with LEC apoptosis, we performed active caspase 3 staining. We found that the percentage of apoptotic LECs in dermal lymphatics was comparable among control and *Rasip1* conditional null embryos at E16.0, suggesting that the fragmented vessel phenotype is likely a direct consequence of defective lymphatic endothelial junctions, rather than increased apoptosis (Fig. S5). Therefore, we started to evaluate the timing and origin of the cell junction defects observed in the mutant embryos by analyzing earlier (E11.5) embryonic stages, before lymphatic vessel formation. At this early stage, an apparently normal number of Prox1-expressing LEC progenitors was seen inside the CV and budding off into the surrounding mesenchyme in the mutant embryos (Fig. S6A,B). These data suggested that loss of *Rasip1* did not affect LEC differentiation and migration at this early stage. However, analysis of LEC junctions in these embryos revealed that VE-cadherin and ZO-1 expression levels were already dramatically reduced at this early stage (Fig. S6). We investigated whether this dramatic reduction in junction molecules could be secondary to changes in cytoskeleton organization or signaling through cell-matrix adhesion. Phalloidin labeling indicated that actin filament organization was apparently normal in *Rasip1* conditional null embryos (Fig. S7A,B). Similarly, no obvious differences in cell-matrix adhesion were detected when using p-Paxillin staining, a

Development (2018) 145, dev165092. doi:10.1242/dev.165092

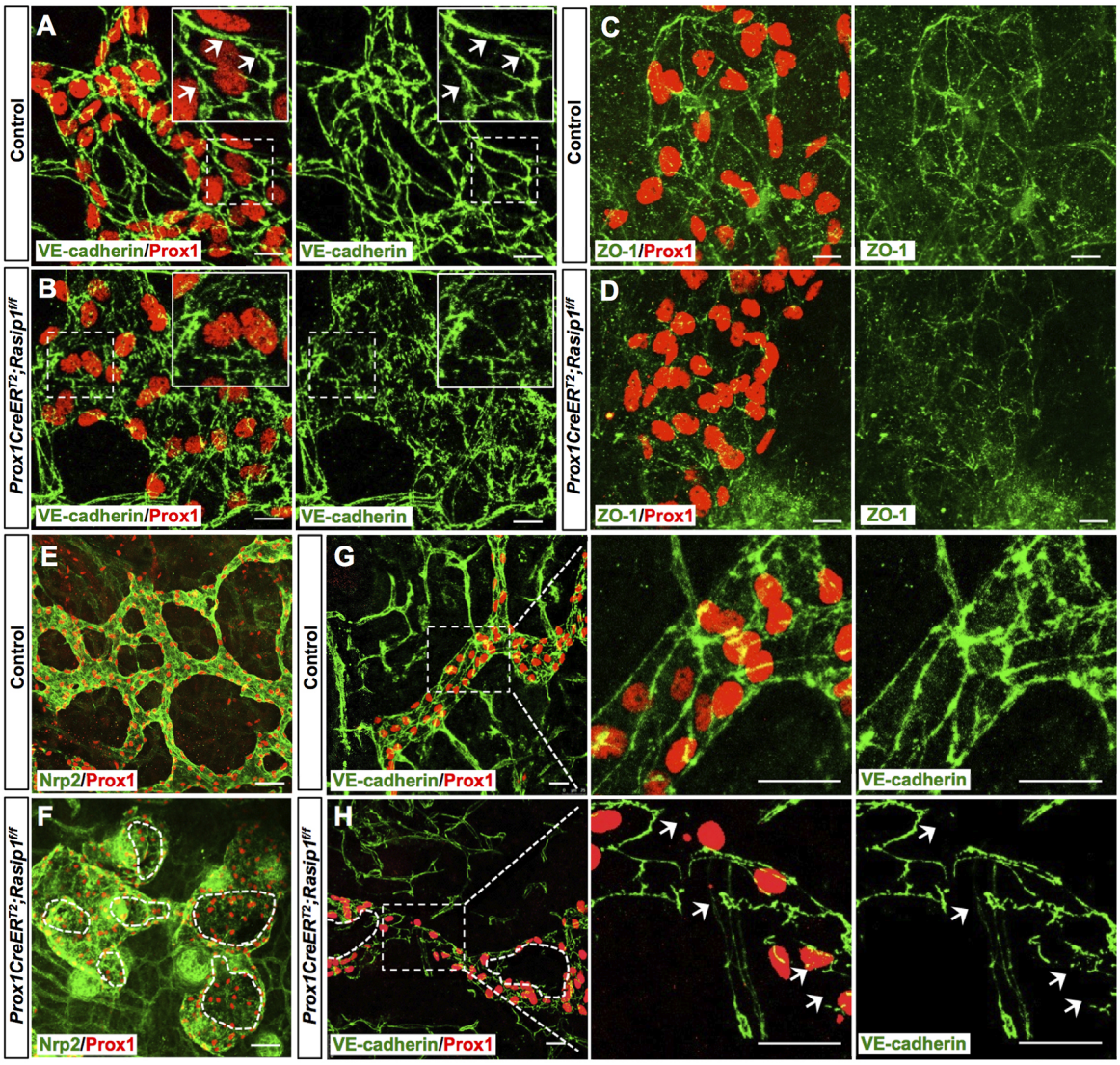

Fig. 3. Disorganized cell junctions in dermal lymphatics of E14.5 *Prox1CreER^{T2};Rasip1$^{f/f}$* embryos. (A,B) Whole-mount immunostaining of dermal lymphatic capillaries from E14.5 control (*n*=4) and *Prox1CreER^{T2};Rasip1$^{f/f}$* (*n*=3) embryos. Insets are higher magnifications of selected regions (dashed boxes). Control lymphatics show zipper-like junctions as indicated by white arrows. Instead, obvious cell junctions are difficult to detect in *Rasip1* conditional null littermates, as cell borders appear to be disorganized and diffuse. (C,D) Similar skin whole-mount immunostaining was performed in control (*n*=3) and *Prox1CreER^{T2};Rasip1$^{f/f}$* (*n*=3) embryos but using antibodies against the tight junction ZO-1 and Prox1. In this case, junctions were also diffuse and defective, and levels of ZO-1 appeared to be reduced. (E-H) Whole-mount immunostaining of dermal lymphatic capillaries from E16 control (*n*=3) and *Prox1CreER^{T2};Rasip1$^{f/f}$* (*n*=3) embryos. Dashed lines indicate open and broken lumens in F and H. Right panels show higher magnifications of the boxed regions in G and H. Arrows indicate the broken junctions in *Rasip1* conditional null embryos. Scale bars: 10 µm in A-D; 50 µm in E,F; 25 µm in G,H.

downstream signaling molecule of focal adhesion kinases (Fig. S7C-E). Together, these results argue that the defective junction integrity observed in *Rasip1* conditional null embryos is likely to be the primary defect caused by the loss of *Rasip1* function.

Rasip1 is required for lymphatic valve formation

As Rasip1 is highly colocalized with Prox1 in lymphatic valve-forming cells (Fig. 1D), we evaluated its functional role in those cells. *Rasip1* conditional null embryos injected with TM at E9.5 and E10.5 die at ∼E16.5, and in addition to the fragmented collecting lymphatic vessel defects, lymphatic valve formation was also severely impaired or missing (Fig. 4F,G). To investigate whether this phenotype was a consequence of a direct role of Rasip1 in lymphatic valve development, or whether it was secondary to the collapsing lymphatics, we injected TM at E14.5, a stage when lymphatic valve formation is starting, and analyzed the mesenteric vessels at E17.5. Whole-mount staining with antibodies against PECAM1, Prox1 and VEGFR3 revealed that V-shaped lymphatic valves were well established in control embryos at this stage (Fig. 5A,B). However, *Rasip1* conditional null embryos showed dilated collecting lymphatic vessels without, or with only a few, lymphatic valves (Fig. 5C-E). This phenotype was further confirmed by whole-mount staining against integrin α9. Integrin α9 has been reported to play an important role in the LEC-ECM signaling required for lymphatic valve formation (Bazigou et al., 2009). Integrin α9 is highly expressed in lymphatic valve regions, but expressed at lower levels in the intermediate lymphangion areas in littermate controls (Fig. 5F). However, in *Rasip1* conditional null embryos, integrin α9 levels were uniformly low along the collecting lymphatic vessels

Development (2018) 145, dev165092. doi:10.1242/dev.165092

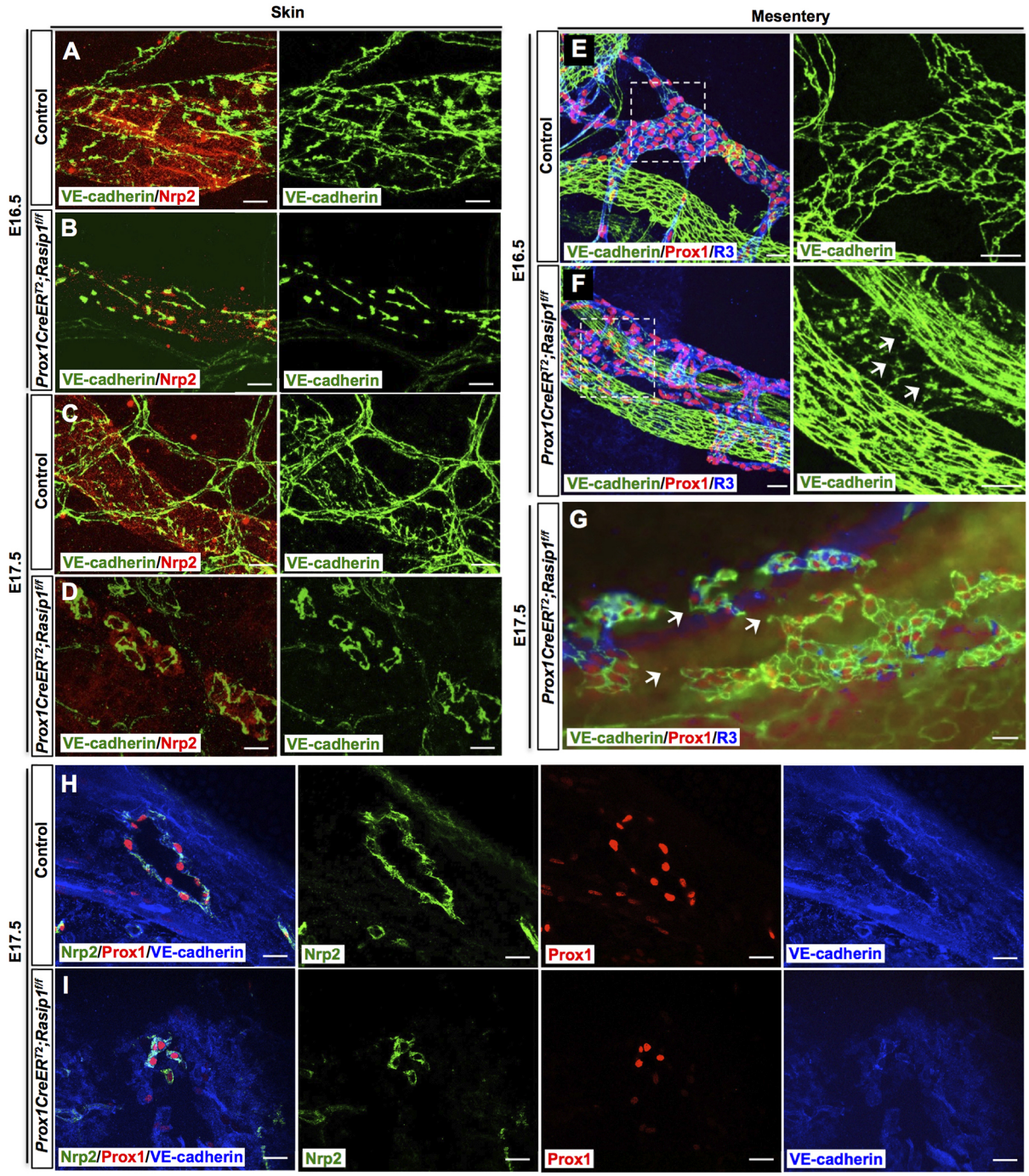

Fig. 4. Impaired lymphatic integrity in *Prox1CreER^{T2};Rasip1$^{f/f}$* embryos at later embryonic stages. (A-D) Whole-mount immunostaining of E16.5 (A,B) and E17.5 (C,D) dermal lymphatics in control and *Prox1CreER^{T2};Rasip1$^{f/f}$* embryos against VE-cadherin and the lymphatic marker Nrp2. Normal morphology and cell junctions are seen in control embryos at those stages, whereas lymphatic vessel integrity appears to be compromised in the mutant embryos, dermal vessels get fragmented and cell junction borders appear to be diffuse and abnormal. (E,F) Whole-mount staining of E16.5 mesentery lymphatics in control (E) and *Prox1CreER^{T2};Rasip1$^{f/f}$* (F) embryos. Right panels show higher magnifications of the boxed regions in E and F. Similar to the dermal lymphatics, VE-cadherin junctions appear to be disorganized in *Prox1CreER^{T2};Rasip1$^{f/f}$* embryos (arrows). (G) At E17.5, the mesenteric lymphatics are severely fragmented, collapsing and losing VE-cadherin expression (arrows) in the mutant embryos. *n*=3 embryos per genotype per stage. TM was induced at E9.5 and E10.5. (H,I) Immunostaining of thicker vibratome sections of control (*n*=3) and *Prox1CreER^{T2};Rasip1$^{f/f}$* (*n*=3) embryos, showing narrow and broken lumens in *Rasip1* conditional null embryos at E17.5, reflecting the fragmented vessels at this stage. Scale bars: 10 µm in A-D; 25 µm in E-I.

without any indication of valve formation (Fig. 5G). The dramatic reduction of integrin α9 levels suggested that LEC-ECM interactions in *Rasip1* conditional null embryos are impaired.

Using the same experimental setting (TM injection at E14.5), we also examined lymphatic vessel junctions in E17.5 collecting lymphatics (Fig. S8A,B) and capillaries (Fig. S8C,D). Similar to the phenotype observed when TM was injected at E9.5 and E10.5 (Fig. 3), collecting lymphatics and lymphatic capillaries were also abnormally dilated with disorganized junctions and reduced VE-cadherin expression levels. These data suggest that Rasip1 is

Development (2018) 145, dev165092. doi:10.1242/dev.165092

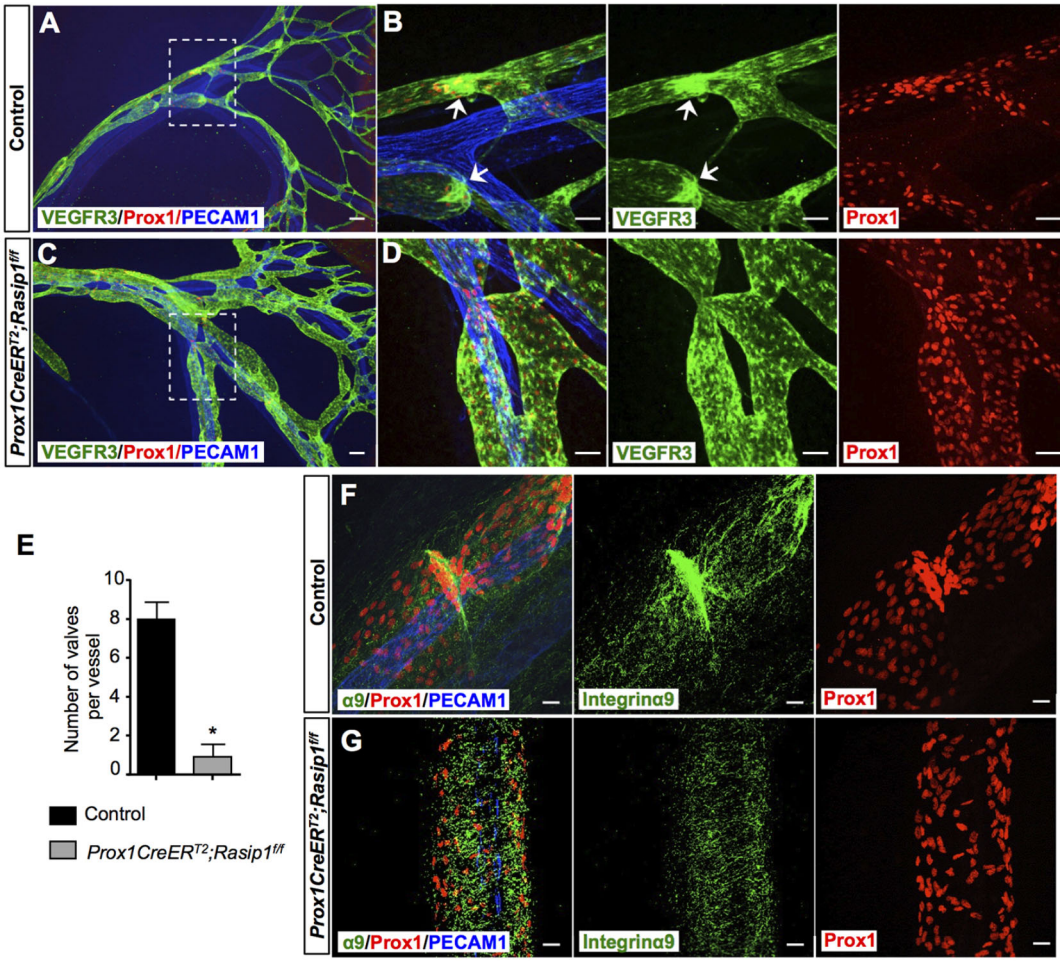

Fig. 5. Impaired valve formation in E17.5 *Prox1CreER^{T2};Rasip1$^{f/f}$* mesenteric lymphatics. (A-D) Whole-mount immunostaining of E17.5 mesentery lymphatic vessels in control (n=3) and *Prox1CreER^{T2};Rasip1$^{f/f}$* (n=3) embryos. B and D are higher magnifications of the boxed regions in A and C, respectively. Valve formation is obvious in control embryos at this stage (arrows). This process appears to be arrested in mutant littermates, as no indication of valve forming regions are detected. (E) Quantification of lymphatic valve numbers in mesenteric lymphatics of control and *Prox1CreER^{T2};Rasip1$^{f/f}$* embryos. Data are derived from six randomly selected fields per genotype. Data are mean±s.e.m. *P<0.05 (Student's t-test, versus control). (F,G) Whole-mount immunostaining of E17.5 control (n=3) and *Prox1CreER^{T2};Rasip1$^{f/f}$* (n=3) mesenteric lymphatics with antibodies against integrin α9, Prox1 and PECAM1 confirms the lack of valves in mutant vessels. Scale bars: 50 µm in A-D; 25 µm in F,G.

required for lymphatic valve development and lymphatic cell junction maintenance.

Rasip1 activity is not required in postnatal lymphatics

Finally, we examined whether Rasip1 was also required for lymphatic lumen and lymphatic valve maintenance. To do this, we induced *Rasip1* deletion at postnatal stages, from postnatal day (P) 0 to P4, and *Rasip1* deletion was examined at P6 (Fig. S9). No obvious lymphatic phenotypes were observed in these conditional mutant pups, as both lymphatic valves (Fig. 6A,B) and lymphatic capillaries (Fig. 6C,D) appeared to be normal. Furthermore, the total number of mature lymphatic valves and the lymphatic vessel caliber in dermal capillaries were comparable with those of control embryos (Fig. 6E,F). These data indicated that Rasip1 is indispensable for early lymphatic morphogenesis, but it is not required for lymphatic valves or lymphatic lumen maintenance during postnatal stages.

Rasip1 regulates LEC junction stability and EC-ECM adhesion by regulating Cdc42 activity

Previous studies demonstrated that, in blood vessels, Rasip1 regulation of VE-cadherin-mediated EC-EC junctions and integrin-mediated EC-ECM junctions is crucial for blood vessel tubulogenesis and blood endothelial junctions (Xu et al., 2011). In these cells, Rasip1 inhibits RhoA, and in turns promotes the activity of Cdc42 and Rac1, to allow controlled expansion of vessel lumens during embryonic growth (Xu et al., 2011; Barry et al., 2016). To evaluate these regulatory pathways in LECs, we carried out an *in vitro* culture approach to remove RASIP1 function and found a significant reduction in CDC42 activity in siRNA-treated human dermal LECs, compared with controls (Fig. 7A). In contrast, the activity of RAC1 and RHOA were not significantly affected (Fig. 7A). These data suggested that Cdc42 is a potential target of Rasip1 in LECs during lymphatic morphogenesis. In fact, previous studies demonstrated that *Cdc42* is essential for maintaining blood vessel stability, by regulating cell-cell junctions and focal adhesions in blood endothelial cells (Barry et al., 2015). Therefore, we next tested whether RASIP1 regulates LEC cell junctions and focal adhesion activities by modulating CDC42 activity. Human dermal LECs were treated with control siRNA (siCtrl), *RASIP1* siRNA (siRasip1) or *CDC42* siRNA (siCdc42). Compared with the control group, LECs treated with siRASIP1 or siCDC42 displayed highly disorganized and reduced adherens junctions (VE-cadherin) and tight junctions (ZO-1)

Development (2018) 145, dev165092. doi:10.1242/dev.165092

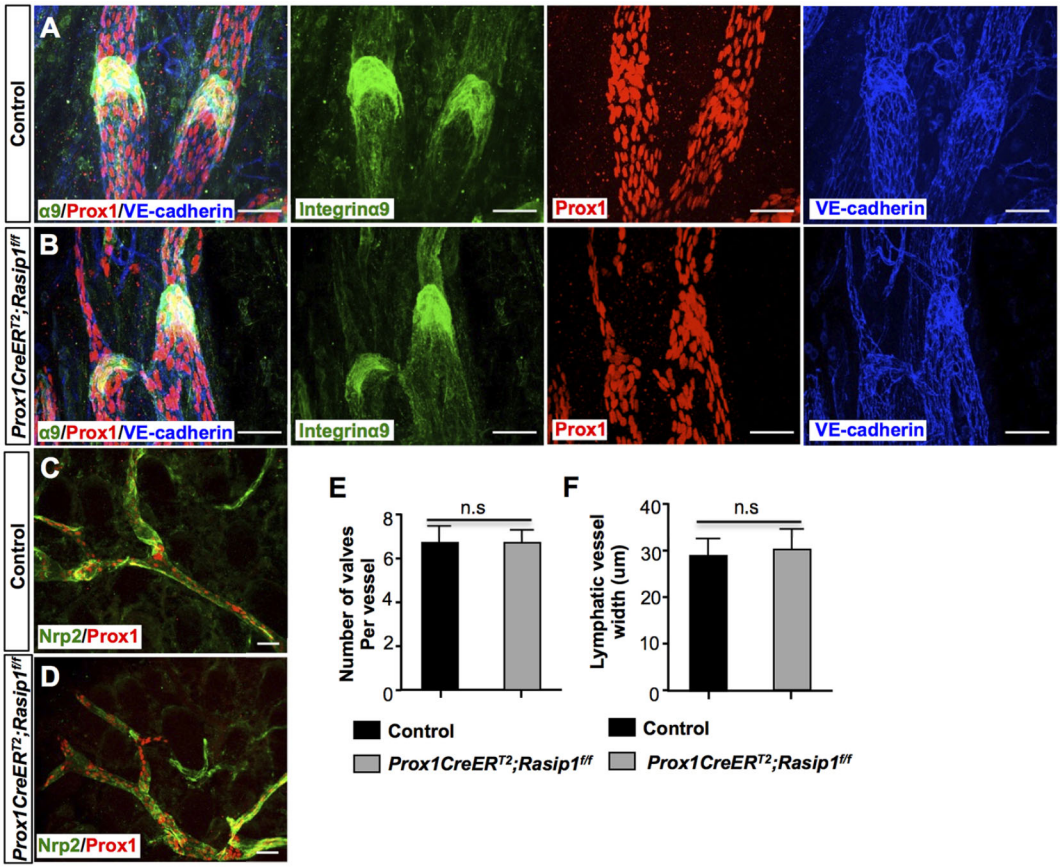

Fig. 6. Rasip1 is not required for lymphatic vessel and lymphatic valve maintenance at later developmental stages. (A,B) Whole-mount staining of P6 mesenteric lymphatic vessels in control (*n*=3) and *Prox1CreER^{T2}; Rasip1$^{f/f}$* (*n*=3) embryos with antibodies against integrin α9, Prox1 and VE-cadherin. TM was induced from P0 to P4. Valve formation appears to be normal in the mutant embryos at this stage. (C,D) Whole-mount staining of P6 dermal lymphatic vessels in control (*n*=3) and *Prox1CreER^{T2};Rasip1$^{f/f}$* (*n*=3) embryos with antibodies against Nrp2 and Prox1. TM was induced from P0 to P4. No obvious changes in lymphatic vessel morphology were observed in the mutant embryos. (E) Quantification of the number of integrin α9^{+} lymphatic valves in control and *Prox1CreER^{T2};Rasip1$^{f/f}$* pups. Data are derived from five randomly selected fields per genotype. (F) Quantification of lymphatic vessel diameter in control and *Prox1CreER^{T2};Rasip1$^{f/f}$* pups. Data are derived from five randomly selected fields per genotype. Data are mean±s.e.m. Student's *t*-test. n.s., not significant. Scale bars: 50 µm.

(Fig. 7B). Previous reports indicated an important role of Cdc42 in regulating the actin cytoskeleton in ECs, and deletion of *Cdc42* in ECs leads to disruptive F-actin organization and EC adhesions (Barry et al., 2015). Therefore, we investigated whether actin organization was impaired in *Rasip1* conditional null embryos. Phalloidin labeling revealed that mesentery lymphatics displayed abnormal punctuated and scattered actin filaments in *Rasip1* conditional null embryos (Fig. S10A,B). Moreover, the intensity of the Phalloidin labeling was reduced overall (Fig. S10C) in *Rasip1* conditional mutants. These data suggested an additional potential regulatory role of Rasip1 in lymphatic actin organization via its regulation of Cdc42 activity in LECs. We therefore tested actin organization in siRASIP1 or siCDC42 treated human dermal LECs *in vitro*. Similar to the *in vivo* situation, siRASIP1- or siCDC42-treated LECs exhibited highly reduced punctuated and abnormal F-actin organization compared with control siRNA-treated groups, as shown by Phalloidin labeling (Fig. S10D,E). Furthermore, cultured human dermal LECs treated with siRASIP1 or siCDC42 exhibited impaired LEC-ECM adhesions, as indicated by reduced p-Paxillin staining (a marker for immature focal adhesion complexes) (Fig. 7C) and active integrin β1 staining (a marker for mature focal adhesions) (Fig. S11). This result suggested a reduction in focal adhesion activities and in LEC-ECM interactions upon *Rasip1* inactivation, further supporting the proposal that Rasip1 regulates LEC-ECM interactions by regulating Cdc42 activity. Similarly, western blot analysis revealed an overall reduction of VE-cadherin, ZO-1 and p-Paxillin levels following siRASIP1 or siCDC42 treatment (Fig. 7D,E). Together, these data indicate that Rasip1 regulates both LEC junction integrity and LEC-ECM adhesion by regulating Cdc42 activity.

Cdc42-deficient embryos phenocopy the lymphatic defects of LEC-specific *Rasip1*-deficient embryos

To further validate the proposal that Rasip1 regulation of Cdc42 activity is responsible for the lymphatic defects identified in *Rasip1* conditional null embryos, we analyzed *Cdc42*-deficient embryos. To do this, we crossed *Cdc42*-floxed mice (Chen et al., 2006) with *Cdh5CreER^{T2}* mice (Wang et al., 2010). Previous work showed that deletion of *Cdc42* with *Tie2Cre* resulted in embryonic lethality between E9.5 and E10.5, because of blood vessels defects; later deletion using *Cdh5CreER^{T2}* induced at E11.5 led to 100% lethality at E14.5 (Barry et al., 2015). To bypass those blood vessel defects, Cre activity was induced at E12.5 and E13.5. In agreement with that previous report (Barry et al., 2015), *Cdh5CreER^{T2}; Cdc42$^{f/f}$* embryos showed widespread hemorrhage and milder edema (Fig. S12A). To examine lymphatic vessel morphogenesis, skin was used for whole-mount immunostaining using antibodies against Nrp2, Prox1 and PECAM1. Similar to *Rasip1* conditional null embryos, E14.5 *Cdc42*-deficient embryos showed dramatically

Development (2018) 145, dev165092. doi:10.1242/dev.165092

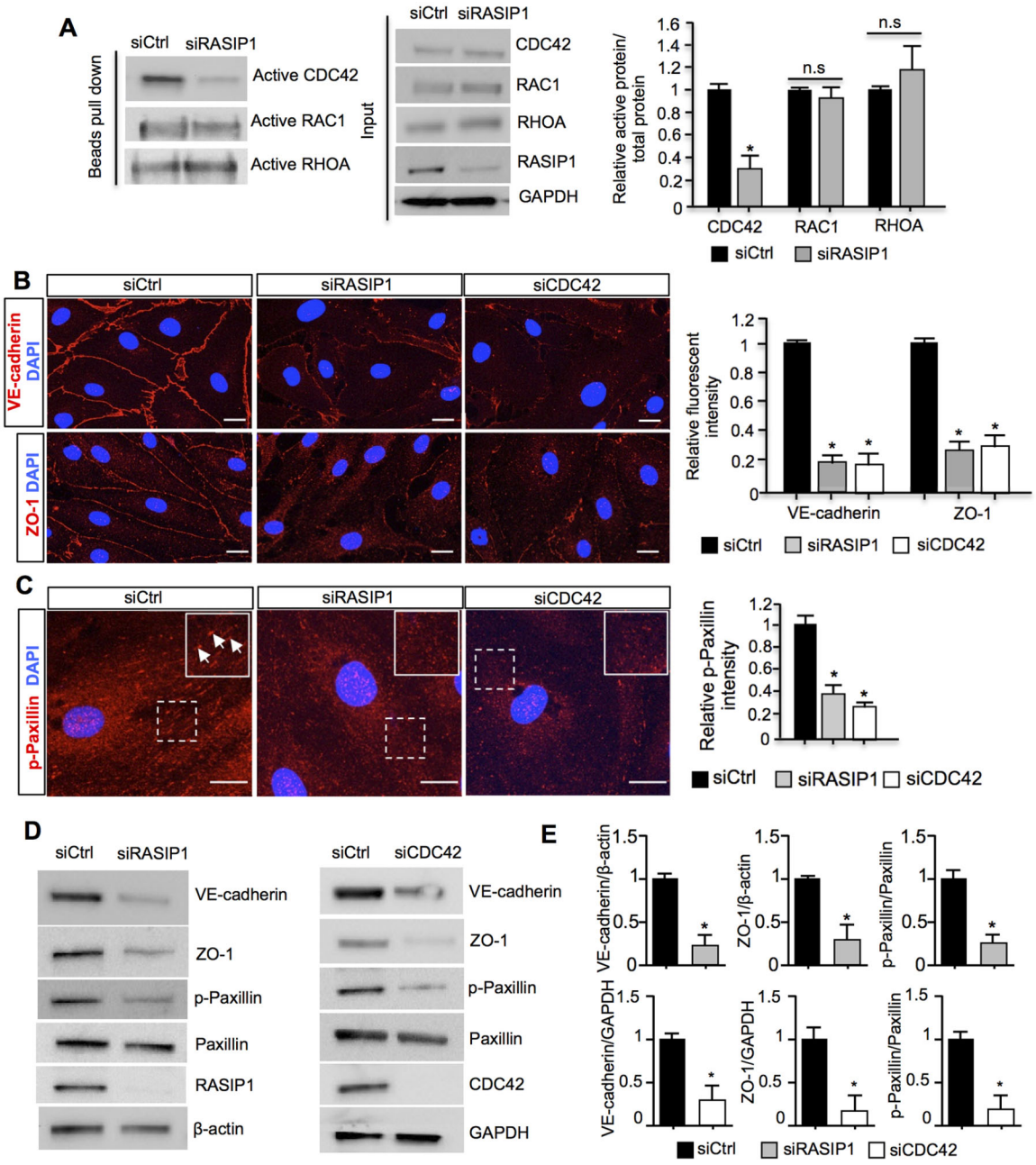

Fig. 7. Rasip1 regulates cell-cell junctions and LEC-ECM junctions by regulating Cdc42 activity in LECs. (A) Western blot analysis of active Rho GTPases (CDC42, RAC1 and RHOA) in siCtrl and siRASIP1-treated human dermal LECs. As seen in the left panel, the level of active CDC42 is severely downregulated in siRASIP1-treated cells. No obvious changes in activity are seen for active RAC1 or RHOA. The total levels of CDC42, RAC1, RHOA, RASIP1 and GAPDH are shown in the middle panel. Quantification of the ratio of active versus total CDC42, RAC1 and RHOA in siCtrl and siRASIP1-treated LECs is shown on the right. Data are mean±s.e.m. of triplicate experiments. **P*<0.05 (Student's *t*-test, versus siCtrl). (B) Immunostaining of siCtrl, siRASIP1- or siCDC42-treated LECs with antibodies against VE-cadherin (upper panel) and ZO-1 (lower panel). The fluorescent intensity of VE-cadherin and ZO-1 from each group were quantified and are shown in the right panel. The levels of VE-cadherin and ZO-1 are drastically reduced in the siRASIP1- or siCDC42-treated LECs. Data are mean±s.e.m. of triplicate experiments. **P*<0.05 (Student's *t*-test, versus siCtrl). (C) Immunostaining of siCtrl, siRASIP1- or siCDC42-treated LECs with antibodies against p-Paxillin. siRASIP1- and siCDC42-treated LECs showed reduced p-Paxillin levels. Insets in red channels show higher magnification of the boxed regions. White arrows indicate p-Paxillin^{+} regions. Quantifications of p-Paxillin levels in siCtrl, siRASIP1- and siCDC42-treated cells are shown on the right. Data are mean±s.e.m. of triplicate experiments. **P*<0.05 (Student's *t*-test, versus siCtrl). (D) Western blot analysis of protein levels in siCtrl, siRASIP1- or siCDC42-treated LECs with antibodies against VE-cadherin, ZO-1, p-Paxillin, Paxillin, RASIP1 and β-actin or GAPDH. (E) Quantification of the western blot analysis shown in D. Data are normalized to the intensity of β-actin or GAPDH in each group. Data are mean±s.e.m. of triplicate experiments. **P*<0.05 (Student's *t*-test, versus siCtrl). Scale bars: 10 µm.

enlarged lymphatic vessels compared with littermate controls (Fig. S12B). Importantly, lymphatic endothelial cell junctions were also very disorganized and abnormal, and the levels of VE-cadherin and ZO-1 expression were severely downregulated (Fig. 8A-D). These data indicated that Cdc42 activity is important for the regulation of lymphatic vessel morphogenesis. Furthermore, to investigate whether Cdc42 activity is also required for lymphatic valve formation, we induced *Cdc42* deletion at E14.5 and E15.5. Similar to *Rasip1* conditional null embryos, *Cdc42*-deficient embryos failed to form lymphatic valves in E17.5 lymphatic

Development (2018) 145, dev165092. doi:10.1242/dev.165092

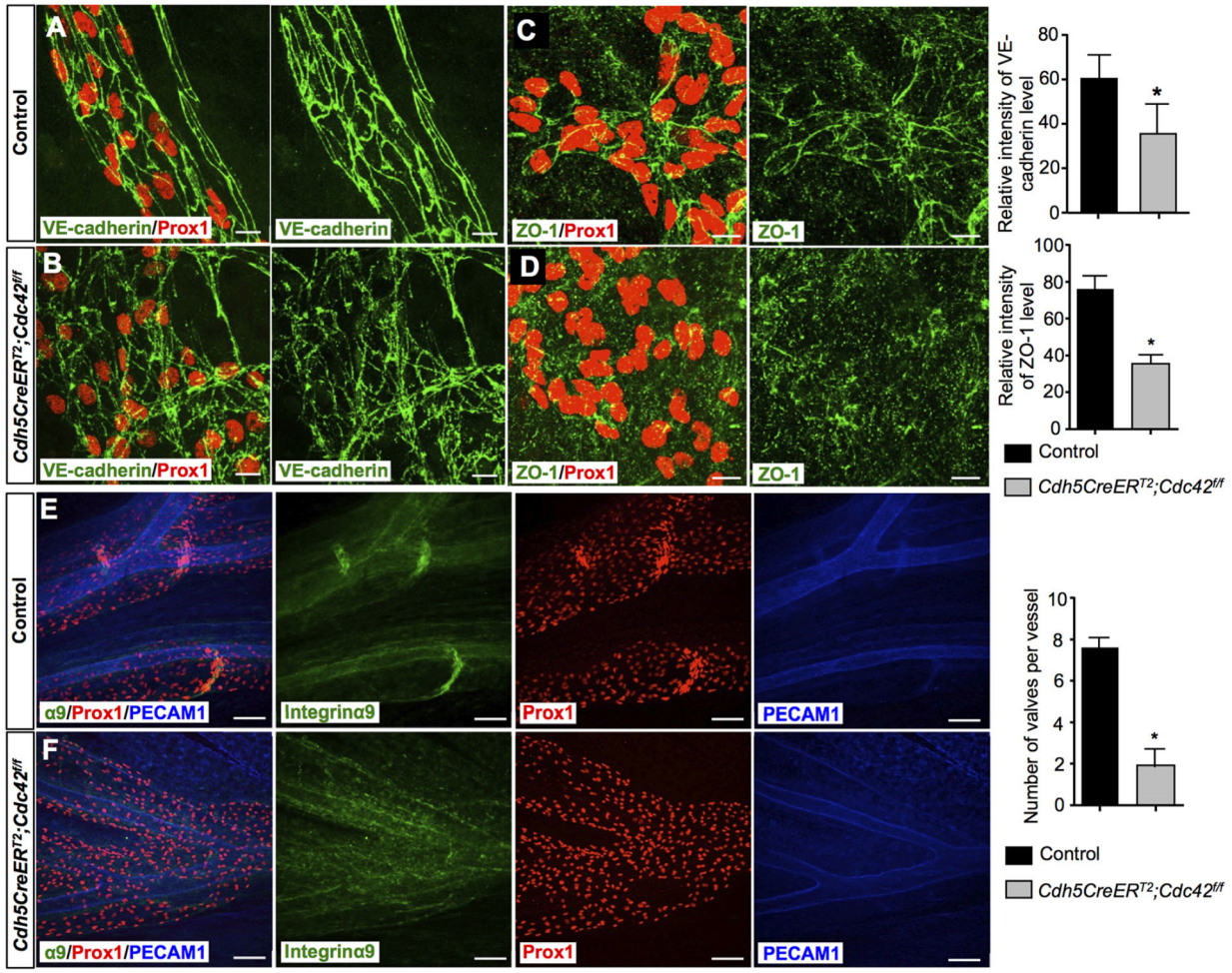

Fig. 8. Abnormal lymphatic endothelial junctions and impaired collecting lymphatic valve formation in *Cdh5CreER^{T2};Cdc42$^{f/f}$* embryos. (A-D) Whole-mount staining of E14.5 dermal lymphatics of control (*n*=3) and *Cdh5CreER^{T2};Cdc42$^{f/f}$* (*n*=3) embryos with antibodies against VE-cadherin and Prox1 (A,B) or ZO-1 and Prox1 (C,D). Cell junctions are diffuse and abnormal in the mutant embryos and levels of VE-cadherin and ZO-1 are downregulated. TM was induced at E12.5 and E13.5. Quantifications of VE-cadherin and ZO-1 levels in both genotypes are shown in the right panel. Data are derived from six randomly selected fields per genotype per experiment. Data are mean±s.e.m. **P*<0.05 (Student's *t*-test, versus control). (E,F) Whole-mount staining of E17.5 mesenteric lymphatics of control (*n*=5) and *Cdh5CreER^{T2};Cdc42$^{f/f}$* (*n*=5) embryos with antibodies against integrin α9, Prox1 and PECAM1. Valve formation is obvious in the control embryos but is missing in the mutant littermates. TM was induced at E14.5 and E15.5. Quantification of number of lymphatic valves in both genotypes is shown on the right. Data are derived from six randomly selected fields per genotype. Data are mean±s.e.m. **P*<0.05 (Student's *t*-test, versus control). Scale bars: 10 µm in A-D; 50 µm in E,F

mesenteries (Fig. 8E,F). Thus, *Cdc42*-deficient embryos phenocopy those lymphatic defects that are observed in *Rasip1* conditional null embryos.

To further support our proposal that Rasip1 regulates Cdc42 activity in LECs, human dermal LECs were treated with control shRNA (shCtrl) or *RASIP1* shRNA (shRASIP1). We then transfected these cells with *CDC42* adenovirus (Cherry-CDC42) or Cherry control adenovirus (Cherry-Ctrl). After 48 h post-transfection, we found that Cherry-CDC42-infected shRASIP1-treated LECs restored their VE-cadherin expression levels and organization (Fig. 9A-C) and exhibited a well-organized cytoskeleton, as visualized by Phalloidin labeling (Fig. 9D-F). These data further support our proposal that, in LECs, Rasip1 regulation of Cdc42 activity is required to maintain proper cell junctions and cytoskeleton organization.

DISCUSSION

Rasip1 conditional null embryos form a lumen

In this study we identified Rasip1 as a key player in lymphatic vasculature lumen formation and maintenance. We show that LEC-specific deletion of *Rasip1* initially leads to dilated lymphatic vessels with enlarged lumens at E14.5. However, these defective lymphatics become disorganized and fragmented at later stages, a phenotype likely because of the dramatic reduction and disorganization of their LEC junctions. Similar to the *in vivo* situation, a reduction of VE-cadherin and ZO-1 levels was observed in cultured LECs upon *RASIP1* inactivation.

Previous work has reported that Rasip1 is essential for blood vasculature lumen formation and/or for its maintenance (Xu et al., 2011; Wilson et al., 2013). One study reported that functional inactivation of *Rasip1* in mice results in null embryos failing to form lumens in blood vessels (Xu et al., 2011). Work by another group argued that blood vessel lumen formation was not affected in *Rasip1*-deficient embryos (Wilson et al., 2013); instead they show that lumens form, but eventually collapse, suggesting that *Rasip1* activity is required for lumen maintenance. Interestingly, our results differ from those that have been reported in blood vessels in various aspects, as *Rasip1* conditional null embryos instead showed dilated lymphatic vessels with enlarged lumens and increased LEC cell

Development (2018) 145, dev165092. doi:10.1242/dev.165092

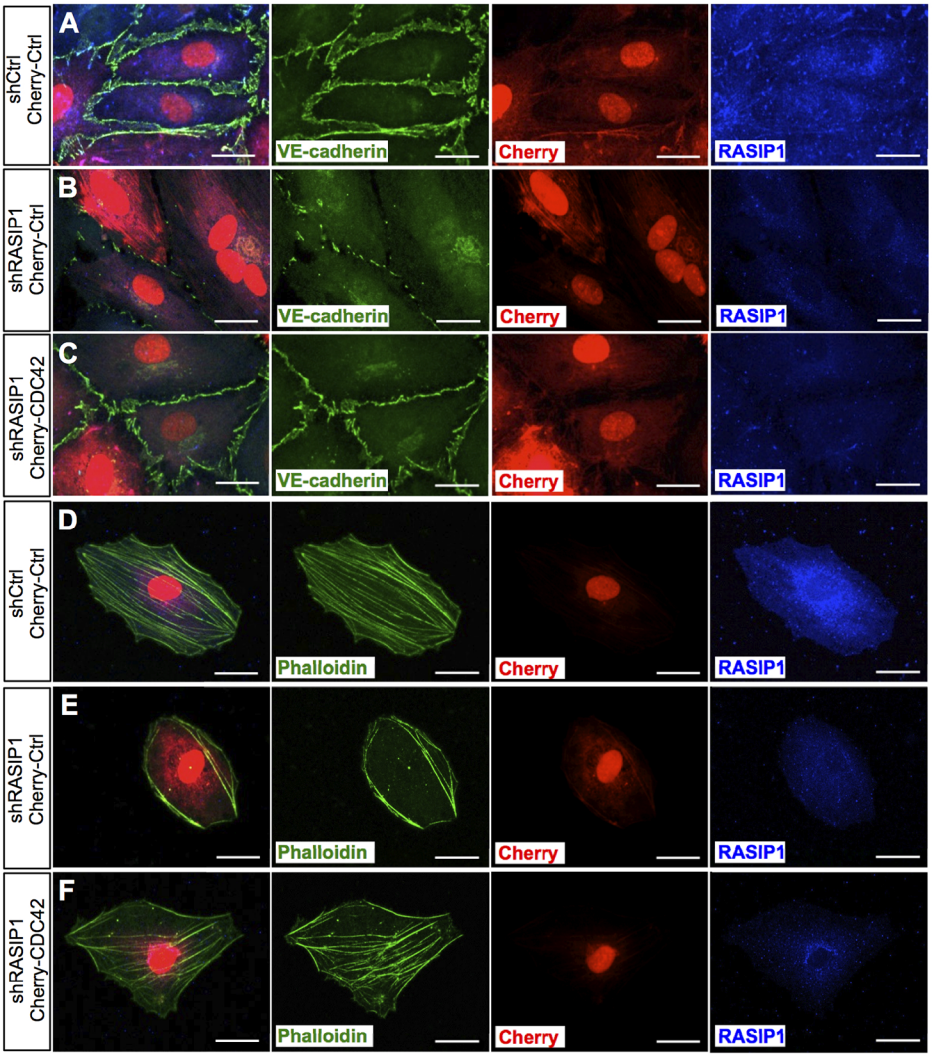

Fig. 9. Ectopic Cdc42 expression restores reduced adhesion junctions and abnormal cytoskeleton organization in *Rasip1*-deficient LECs. (A-C) Human dermal LECs were transfected with shCtrl or shRasip1. After 24 h post-transfection, these cells were further transfected with control adenovirus (Cherry-Ctrl) or Cdc42 adenovirus (Cherry-Cdc42) for two more days. *Rasip1*-deficient LECs (shRasip1-treated LECs) showed impaired adhesion junctions with decreased VE-cadherin levels (B). Ectopic *Cdc42* expression restored VE-cadherin levels in *Rasip1*-deficient LECs (C). (D-F) *Rasip1*-deficient LECs (shRasip1 treated LECs) showed decreased F-actin fibers (E). Ectopic *Cdc42* expression restored F-actin levels in *Rasip1*-deficient LECs (F). Scale bars: 10 µm.

numbers at E14.5. We showed that this dilation is because of increased LEC proliferation that is concomitant with a reduction in the level of VE-cadherin expression. Previous studies showed that blocking VE-cadherin activity increases proliferation in ECs (Nelson and Chen, 2003). Therefore, the observed increase in LEC proliferation could be due to the dramatic reduction in the level of VE-cadherin expression in *Rasip1* conditional null embryos.

Rasip1 regulation of lymphatic endothelial cell junction integrity is required for lymphatic lumen maintenance

Mature lymphatic capillaries have been described as having button-like, loose overlapping cell-cell junctions that facilitate the uptake of interstitial fluid into the lymphatic system. However, during early embryonic development, lymphatic capillaries exhibit non-permeable zipper-like junctions that eventually become permeable button-like junctions at later embryonic stages (Yao et al., 2012; Zheng et al., 2014). Failure in this transition, at least in part, contributes to edema and abnormal fluid drainage capacity (Zheng et al., 2014). Interestingly, dermal and mesenteric lymphatics of *Rasip1* conditional null embryos were dramatically disorganized at E16.5 and, one day later, they appeared to be fragmented and collapsed. Importantly, LEC junctions were also very disorganized and abnormal, and their levels of VE-cadherin and ZO-1 expression were severely downregulated. These results indicated that Rasip1 is required for proper cell junction organization and, therefore, for lymphatic lumen maintenance. In addition, we found that LECs in these vessels showed disorganized subcellular F-actin localization. Accordingly, it is likely that the discontinued and broken vessels seen at later stages are a consequence of the impaired junction organization that has already occurred by E14.5.

Rasip1 activity is required for lymphatic valve formation

One of the major characteristics of collecting lymphatic vessels is the presence of lymphatic valves, which prevent retrograde lymph flow and ensure a unidirectional lymph flow back to the blood circulation. Recent studies have identified key genes and the mechanical flow that regulate lymphatic valve formation (Koltowska et al., 2013). Deletion of *Rasip1* in LECs at early embryonic stages results in fragmented and discontinued collecting lymphatic vessels, and these vessels fail to form lymphatic valves. Deletion of *Rasip1* at E14.5, a stage when lymphatic valve formation starts, resulted in impaired lymphatic valve formation, which suggested that Rasip1 regulates this process. More importantly, we found that the level of integrin α9 was dramatically decreased in collecting lymphatic vessels of *Rasip1* conditional null embryos. Interaction of integrin α9 with the ECM is required for proper lymphatic valve formation (Bazigou et al., 2009).

Development (2018) 145, dev165092. doi:10.1242/dev.165092

Thus, failure in lymphatic valve formation in *Rasip1* conditional null embryos is likely because of impaired interactions of LECs with the ECM. This finding is consistent with previous studies showing that Rasip1 regulates EC integrin-dependent adhesion to surrounding ECM during blood vessel lumen formation (Xu et al., 2011).

Cdc42 is a likely direct mediator of Rasip1 function in LECs

We also found that loss of *Rasip1* dramatically abolished Cdc42 activity *in vitro* and *in vivo*, suggesting that Cdc42 is the potential downstream effector of Rasip1 function. In addition, *Rasip1* deletion also led to reduced and abnormal organized F-actin *in vivo* and *in vitro*. This phenotype is different from that reported in BECs, showing that F-actin (RhoA dependent) was significantly increased in *Rasip1*-deficient cells (Xu et al., 2011). This discrepancy is presumably due to the fact that RhoA activity is dramatically increased by *Rasip1* loss in BECs; however, we did not observe significant changes in RhoA activity, but a dramatic reduction in Cdc42 activity in LECs. Therefore, these data suggested an additional potential regulatory role of Rasip1 in lymphatic actin organization, via its regulation of Cdc42 activity in LECs. Conversely, our data

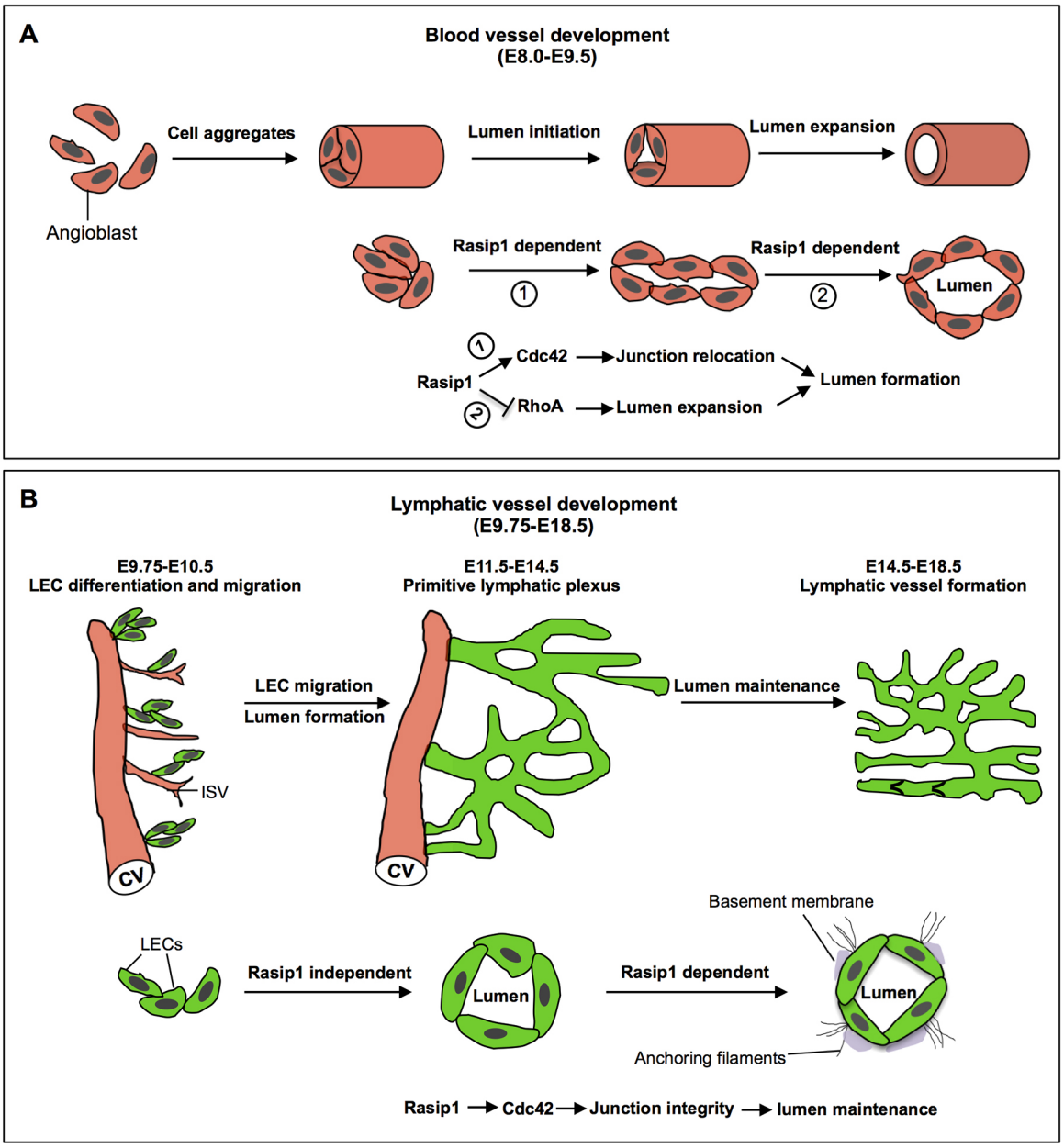

Fig. 10. Schematic view of the role of *Rasip1* in lumen formation and maintenance in blood and lymphatic vessels. (A) Schematic view of blood vessel vasculogenesis at early embryonic stages in mice. Single angioblasts aggregate to form linear cords. Cord-to-tube transition involves a series of cellular changes from lumen initiation to lumen expansion, including junction molecule re-localization and distribution. Rasip1 is required in these processes to clear the adhesions from the apical membrane, to form a single continuous lumen, by temporally regulating different pools of Rho GTPases. (B) Schematic view of lymphatic vessel development during embryonic stages in mice. LECs bud off from the CV as LEC aggregates that already have a lumen; these eventually separate from the venous system and form a mature lymphatic network. Blood vessel lumen formation is a stepwise process and Rasip1 activity is required for lumen formation and maintenance. Instead, lymphatic vessel lumen formation is a rather passive process that occurs as LECs migrate and form the lymphatic network. Therefore, in lymphatics, Rasip1 is not required for lymphatic vessel lumen formation, but it is necessary for lumen maintenance during embryonic developmental stages.

Development (2018) 145, dev165092. doi:10.1242/dev.165092

agreed with previous work showing that Cdc42 regulates F-actin organization and EC adhesions (Barry et al., 2015). Similarly, we found that siRNA knockdown of *Rasip1* or *Cdc42* affected the LEC cytoskeleton and lymphatic endothelial cell adhesions. Focal adhesion kinases have been established as a key component of the signal transduction pathways triggered by integrins (Guan, 1997). We determined that siRNA knockdown of *Rasip1* or *Cdc42* significantly reduced the focal adhesion markers p-Paxillin and active integrin β1 in LECs. Moreover, ectopic Cdc42 expression greatly restored F-actin organization and focal adhesions in *Rasip1*-deficient LECs, further supporting the proposal that Cdc42 activity is regulated by Rasip1.

More importantly, we showed that *Cdc42*-deficient embryos exhibited enlarged lymphatic vessels with disorganized lymphatic endothelial junctions at E14.5. These embryos also failed to form collecting lymphatic valves. Together, these defects largely phenocopied those observed in *Rasip1* conditional null embryos. Accordingly, based on our *in vivo* and *in vitro* data, we argue that Rasip1 regulation of Cdc42 activity is required for cytoskeleton organization and regulation of LEC junctions and LEC-ECM interactions during lymphatic vessel development (Fig. S13). In blood vessel lumen formation, Rasip1 controls a pool of GTPases, such that Rasip1 and its binding partner, the GTPase-activating protein Arhgap29, promotes the activation of Pak4 by Cdc42, which in turn activates NMII (Barry et al., 2016). In the case of lymphatics, we still do not know about the downstream signaling pathways which are regulated by Cdc42 that are required to maintain cell junctions and, therefore, lymphatic vessel and lymphatic lumen integrity.

Taken together, our data support a somewhat different role for Rasip1 during lymphatic vessel development than the one which has been reported during blood vessel formation (Xu et al., 2011). We predict that Rasip1 plays different roles in these two different types of vessels, because of the important differences in the timing and mechanisms controlling lumen formation in these two vasculature networks. Vasculogenesis occurs at early embryonic stages (E8-E9 in the mouse) and single angioblasts aggregate to form continuous cords. The cord-to-tube transition involves a series of cellular changes that are required for lumen initiation and lumen expansion, including junction molecule re-localization and distribution. Rasip1 is required in these processes by temporally regulating different pools of Rho GTPases to clear the adhesions from the apical membrane to form a single, continuous lumen (Xu et al., 2011; Barry et al., 2016) (Fig. 10A). In contrast, the majority of mammalian LECs originate from the CV and intersomitic vessels (ISVs) at ∼E9.75. As these LECs bud off from the CV, they remain attached together by high levels of VE-cadherin. These LECs migrate away from the CV in clusters attached by multiple junctions containing narrow lumens (Fig. 10B). The presence and expansion of these lumens could be due to the fluid flowing through the remaining connections between budding LECs and the CV, such that anchoring filaments eventually sense changes in fluid pressure and/or other yet unknown physiological causes. Blood vessel lumen formation is a stepwise process controlled by the temporal regulation of Rasip1, whereas lymphatic vessel lumen formation is rather a passive process, taking place concomitant with the process of early LEC migration and proliferation. Accordingly, Rasip1 is not required for lymphatic lumen formation, but is necessary for lymphatic vessel lumen maintenance during embryonic stages.

MATERIALS AND METHODS

Mice handling and inducible deletion of *Rasip1* and *Cdc42*

Rasip1-floxed mice (Xu et al., 2011) were generated by Ondine Cleaver's group (UT Southwestern, Dallas, TX, USA); *Lyve1eGFPCre* mice (Pham et al., 2010) were purchased from the Jackson Laboratory; *Cdh5CreER^{T2}* mice were obtained from Ralf H. Adams's group (Wang et al., 2010) (Max Planck Institute for Molecular Biomedicine, Münster, Germany); *Prox1CreER^{T2}* mice have previously been described (Srinivasan et al., 2007). *Rasip1* conditional null embryos were generated by crossing *Rasip1*-floxed mice with *Prox1CreER^{T2}* mice. In general, 2-month- to 8-month-old male and female mice were used for mating and breeding. Mice were backcrossed into the NMRI background for five generations. For deletion of *Rasip*1 in LECs, pregnant mothers were injected intraperitoneally with 5 mg TM per 40 g mouse at E9.5 and E10.5, to examine lymphatic defects at E14.5, E15.5, E16.5 and E17.5. To study the role of Rasip1 in lymphatic valve development, pregnant mothers were injected intraperitoneally with 5 mg TM per 40 g mouse at E14.5. To study the role of Rasip1 in postnatal lymphatic development, control and Rasip1 conditional null neonates received 20 µg of TM per day from P0 to P4 by oral delivery. *Cdc42* conditional null embryos were generated by crossing *Cdc42*-floxed mice (Chen et al., 2006) with *Cdh5CreER^{T2}* mice (Wang et al., 2010) in a CD1 background. To delete *Cdc42*, pregnant mothers were gavaged with 3 mg TM per 40 g mouse either at E12.5 and E13.5 for embryos harvested at E14.5, or at E14.5 and E15.5 for embryos harvested at E17.5. At least three litters per stage were used to assess each time point. All animal husbandry was performed in accordance with protocols approved by Northwestern University and UT Southwestern Medical Center Institutional Animal Care and Use Committee.

Immunofluorescent staining

Cryosections

Embryos were washed with ice-cold PBS and fixed in 4% PFA in the cold room at 4°C overnight and then dehydrated in 30% sucrose. Embryos were embedded in Tissue-Tek O.C.T (Sakura) and 10 µm thick cryosections were used for immunostaining. Sections were washed with PBS and blocked for 1 h at room temperature. Primary antibodies were incubated at 4°C overnight. Secondary antibodies were incubated for 2 h at room temperature. Slides were washed with TBST (Tris-based saline+1% Tween 20) and mounted using mounting medium containing DAPI.

Vibratome sections

Immunostaining was performed as has previously been described (Yang et al., 2012). Briefly, fixed embryos were embedded in 7% low melting point agarose and 100 µm sections were collected for immunostaining. Immunostaining was performed as described above.

Whole-mount staining

Skin and mesentery were isolated at the stages described in the results section and fixed with 4% paraformaldehyde (PFA) overnight or 30 min at room temperature, respectively. Fixed tissues were washed with PBS and blocked at 4°C overnight. Primary antibodies were incubated at 4°C overnight and then tissues were washed with PBST (phosphate-buffered saline+0.1% Triton). Secondary antibodies were incubated for 2 h at room temperature. Tissues were washed with PBST and then mounted with mounting medium containing DAPI.

Cell culture

Cells were washed with PBS and fixed with 4% PFA for 30 min. Immunostaining was performed as described above.

Antibodies

The following primary antibodies were used: rabbit anti-Prox1 (11002, 1:500, AngioBio); goat anti-Prox1 (AF2727, 1:200, R&D Systems); rat anti-PECAM1 (553370, 1:100, BD Pharmingen); goat anti-Lyve1 (AF2125, 1:200, R&D Systems); rat anti-VE-cadherin (clone: 11D4.1, 555289, 1:200, BD Pharmingen); rat anti-VE-cadherin (clone: BV13A, 1:200, ImClone Systems); rabbit anti-VE-cadherin (ab33168, 1:500, Abcam); goat anti-integrin α9 (AF3827, 1:100, R&D Systems); goat anti-VEGFR3 (AF743, 1:100, R&D Systems); goat anti-Nrp2 (AF567, 1:500, R&D Systems); rabbit anti-ZO-1 (40-2200, 1:200, Invitrogen); rabbit anti-Ki67 (clone: SP6, MA5-14520, 1:200, Invitrogen); rabbit anti-active caspase 3 (clone: C92-605, 559565, 1:200, BD Pharmingen); mouse anti-

Development (2018) 145, dev165092. doi:10.1242/dev.165092

paxillin (clone: 349, 610051, 1:200, BD Transduction Laboratories); rat anti-integrin β1 (clone: 9EG7, 550531, 1:200, BD Biosciences); rabbit-anti p-paxillin (2541, 1:500, Cell Signaling Technology); goat anti-Rasip1 (ab21018, 1:500, Abcam); mouse anti-Rac1 (ARC03, 1:100, Cytoskeleton); Cdc42 (ACD03,1:100, Cytoskeleton); RhoA (ARH04, 1:100, Cytoskeleton); rabbit anti-Gapdh (clone: 6C5, sc-32233, 1:1000, Santa Cruz Biotechnology). The following secondary antibodies were used: Alexa 488-conjugated donkey anti-rabbit (A-21206, 1:300, Invitrogen); Alexa 488-conjugated donkey anti-goat (A-11055, 1:300, Invitrogen); Alexa 488-conjugated donkey anti-rat (A-21208, 1:300, Invitrogen); Cy3-conjugated donkey anti-rabbit (711-165-152, 1:300, Jackson ImmunoResearch); Cy3-conjugated donkey anti-mouse (715-165-151, 1:300, Jackson ImmunoResearch); Cy3-conjugated donkey anti-goat (705-165-147, 1:300, Jackson ImmunoResearch); Cy5-conjugated donkey anti-goat (705-495-147, 1:300, Jackson ImmunoResearch) and Cy5-conjugated donkey anti-rat (712-175-150, 1:300, Jackson ImmunoResearch).

siRNA transfection

Human dermal LECs were purchased from PromoCell and cultured in endothelial basal medium (EBM) complemented with supplement mix (C-39225, PromoCell) according to the supplier's instructions. Human *RASIP1* siRNA or *CDC42* siRNAs were obtained from GE Dharmacon and were transfected into cultured human dermal LECs using Lipofectamine 2000 (Thermo Fisher Scientific) as has previously been described (Srinivasan et al., 2014). After 48 h post-transfection, cells were either harvested for western blot or fixed with 4% PFA for immunostaining.

Virus transfection

RASIP1 shRNA lentivirus and control shRNA lentivirus were purchased from OriGene. Cherry-CDC42 adenovirus and Cherry-Control adenovirus were obtained from Dr Gorge Davis's laboratory (University of Missouri School of Medicine, Columbia, USA). *RASIP1* transfection was performed according to the manufacturer's instructions. Briefly, P4 human dermal LECs were cultured to 30% confluence and either *RASIP1* shRNA lentivirus or control lentivirus was added into culture medium containing 8 µg/ml Polybrene (Sigma-Aldrich). After 24 h post-transfection, cells were changed into EBM basal medium and *CDC42* adenovirus transfection was performed as has previously been described (Norden et al., 2016). Two days after infection, cells were fixed with 4% PFA for immunostaining.

In vitro GTPase pull-down assays

Rho GTPase activity was detected by using the RHOA/RAC1/CDC42 Activation Assay Combo Biochem Kit (Cytoskeleton). Briefly, cultured control siRNA- and *RASIP1* siRNA-treated human dermal LECs were lysed using ice-cold cell lysis buffer supplemented with 1× protease inhibitor cocktail (Roche) on ice for 30 min according to the manufacturer's instruction (Cytoskeleton). Cell lysates from control siRNA and *RASIP1* siRNA treated LECs were incubated with rhotekin-RBD (for RHOA activation assay) or PAK- PBD beads (for RAC1 and CDC42 activation assays) for 1 hour at 4°C. Beads were centrifuged and washed four times with washing buffer and eluted with 2× Laemmli sample buffer. Bound active CDC42/RAC1 or RHOA proteins were detected by western blot. In separate experiments, 20-50 µg of cell lysates from each sample were used to determine total RHOA, RAC1 or CDC42 by western blot.

Image analysis

Whole-mount samples and vibratome tissue sections were immunostained and then visualized with a confocal laser-scanning microscope (Zeiss LSM510). For images to be compared quantitatively, the same laser intensity settings were used and images were acquired on the same day. Quantification of the fluorescence intensity was performed using ImageJ. The identity of LECs was defined by Prox1 staining and the LEC boundaries were outlined using ImageJ. Images were transformed to 8-bit grayscale. Regions of interest were selected manually by using the section tools, and the mean fluorescent intensity of the selected areas was measured after background subtraction. For quantification, at least three regions of interest were selected and mean values were quantified for each image. The numbers of samples in each group and the statistical analysis, are listed in the individual figure legends.

Acknowledgements

We thank Ralf H. Adams for the *Cdh5CreER^{T2}* mice. We thank all the members in G.O.'s and Beatriz Sosa-Pineda's laboratories for invaluable discussions. We thank Benjamin R. Thomson and Isabel A. Carota for skilled technical help. We thank Donald McDonald and Peter Baluk for valuable comments.

Competing interests

The authors declare no competing or financial interests.

Author contributions

Conceptualization: X.L., G.O.; Methodology: X.L., M.O., H.J.G.; Validation: X.L., H.J.G.; Formal analysis: X.L.; Investigation: X.L., W.M., M.O.; Resources: X.G., W.M., G.E.D., O.C., G.O.; Writing - original draft: X.L., G.O.; Supervision: G.O.; Funding acquisition: G.O.

Funding

This work was supported by the National Institutes of Health (grants RO1HL073402-16 to G.O., RO1HL126518 to O.C. and the National Research Service Award T32 training grant 1T32HL134633-01A1 to X.L.). Deposited in PMC for release after 12 months.

Supplementary information

Supplementary information available online at
http://dev.biologists.org/lookup/doi/10.1242/dev.165092.supplemental

References

Aitsebaomo, J., Wennerberg, K., Der, C. J., Zhang, C., Kedar, V., Moser, M., Kingsley-Kallesen, M. L., Zeng, G. Q. and Patterson, C. (2004). p68RacGAP is a novel GTPase-activating protein that interacts with vascular endothelial zinc finger-1 and modulates endothelial cell capillary formation. *J. Biol. Chem.* **279**, 17963-17972.

Alitalo, K. (2011). The lymphatic vasculature in disease. *Nat. Med.* **17**, 1371-1380.

Aspelund, A., Tammela, T., Antila, S., Nurmi, H., Leppänen, V. M., Zarkada, G., Stanczuk, L., Francois, M., Mäkinen, T., Saharinen, P. et al. (2014). The Schlemm's canal is a VEGF-C/VEGFR-3-responsive lymphatic-like vessel. *J. Clin. Invest.* **124**, 3975-3986.

Barry, D. M., Xu, K., Meadows, S. M., Zheng, Y., Norden, P. R., Davis, G. E. and Cleaver, O. (2015). Cdc42 is required for cytoskeletal support of endothelial cell adhesion during blood vessel formation in mice. *Development* **142**, 3058-3070.

Barry, D. M., Koo, Y., Norden, P. R., Wylie, L. A., Xu, K., Wichaidit, C., Azizoglu, D. B., Zheng, Y., Cobb, M. H., Davis, G. E. et al. (2016). Rasip1-mediated Rho GTPase signaling regulates blood vessel tubulogenesis via nonmuscle myosin II. *Circ. Res.* **119**, 810-826.

Bazigou, E., Xie, S., Chen, C., Weston, A., Miura, N., Sorokin, L., Adams, R., Muro, A. F., Sheppard, D. and Makinen, T. (2009). Integrin-α9 is required for fibronectin matrix assembly during lymphatic valve morphogenesis. *Dev. Cell.* **17**, 175-186.

Chen, L., Liao, G., Yang, L., Campbell, K., Nakafuku, M., Kuan, C.-Y. and Zheng, Y. (2006). Cdc42 deficiency causes Sonic hedgehog-independent holoprosencephaly. *Proc. Natl. Acad. Sci. USA* **103**, 16520-16525.

Chen, X.-G., Lv, Y.-X., Zhao, D., Zhang, L., Zheng, F., Yang, J.-Y., Li, X.-L., Wang, L., Guo, L.-Y., Pan, Y. et al. (2016). Vascular endothelial growth factor-C protects heart from ischemia/reperfusion injury by inhibiting cardiomyocyte apoptosis. *Mol. Cell. Biochem.* **413**, 9-23.

Connolly, J. O., Simpson, N., Hewlett, L. and Hall, A. (2002). Rac regulates endothelial morphogenesis and capillary assembly. *Mol. Biol. Cell.* **13**, 2474-2485.

Gordon, E. J., Gale, N. W. and Harvey, N. L. (2008). Expression of the hyaluronan receptor LYVE-1 is not restricted to the lymphatic vasculature; LYVE-1 is also expressed on embryonic blood vessels. *Dev. Dyn.* **237**, 1901-1909.

Guan, J.-L. (1997). Role of focal adhesion kinase in integrin signaling. *Int. J. Biochem. Cell Biol.* **29**, 1085-1096.

Harvey, N. L., Srinivasan, R. S., Dillard, M. E., Johnson, N. C., Witte, M. H., Boyd, K., Sleeman, M. W. and Oliver, G. (2005). Lymphatic vascular defects promoted by Prox1 haploinsufficiency cause adult-onset obesity. *Nat. Genet.* **37**, 1072-1081.

Henri, O., Pouehe, C., Houssari, M., Galas, L., Nicol, L., Edwards-Lévy, F., Henry, J.-P., Dumesnil, A., Boukhalfa, I., Banquet, S. et al. (2016). Selective Stimulation of cardiac lymphangiogenesis reduces myocardial edema and fibrosis leading to improved cardiac function following myocardial InfarctionCLINICAL PERSPECTIVE. *Circulation* **133**, 1484-1497.

Ikram, M. K., Sim, X., Xueling, S., Jensen, R. A., Cotch, M. F., Hewitt, A. W., Ikram, M. A., Wang, J. J., Klein, R., Klein, B. E. K. et al. (2010). Four novel Loci (19q13, 6q24, 12q24, and 5q14) influence the microcirculation in vivo. *PLoS Genet.* **6**, e1001184.

Kizhatil, K., Ryan, M., Marchant, J. K., Henrich, S. and John, S. W. M. (2014). Schlemm's canal is a unique vessel with a combination of blood vascular and lymphatic phenotypes that forms by a novel developmental process. *PLoS Biol.* **12**, e1001912.

Klotz, L., Norman, S., Vieira, J. M., Masters, M., Rohling, M., Dubé, K. N., Bollini, S., Matsuzaki, F., Carr, C. A. and Riley, P. R. (2015). Cardiac lymphatics are heterogeneous in origin and respond to injury. *Nature* **522**, 62-67.

Koltowska, K., Betterman, K. L., Harvey, N. L. and Hogan, B. M. (2013). Getting out and about: the emergence and morphogenesis of the vertebrate lymphatic vasculature. *Development* **140**, 1857-1870.

Komatsu, M. and Ruoslahti, E. (2005). R-Ras is a global regulator of vascular regeneration that suppresses intimal hyperplasia and tumor angiogenesis. *Nat. Med.* **11**, 1346-1350.

Koo, Y., Barry, D. M., Xu, K., Tanigaki, K., Davis, G. E., Mineo, C. and Cleaver, O. (2016). Rasip1 is essential to blood vessel stability and angiogenic blood vessel growth. *Angiogenesis* **19**, 173-190.

Louveau, A., Smirnov, I., Keyes, T. J., Eccles, J. D., Rouhani, S. J., Peske, J. D., Derecki, N. C., Castle, D., Mandell, J. W., Lee, K. S. et al. (2015). Structural and functional features of central nervous system lymphatic vessels. *Nature* **523**, 337-341.

Ma, W. and Oliver, G. (2017). Lymphatic endothelial cell plasticity in development and disease. *Physiology* **32**, 444-452.

Mitin, N. Y., Ramocki, M. B., Zullo, A. J., Der, C. J., Konieczny, S. F. and Taparowsky, E. J. (2004). Identification and characterization of rain, a novel Ras-interacting protein with a unique subcellular localization. *J. Biol. Chem.* **279**, 22353-22361.

Nelson, C. M. and Chen, C. S. (2003). VE-cadherin simultaneously stimulates and inhibits cell proliferation by altering cytoskeletal structure and tension. *J. Cell Sci.* **116**, 3571-3581.

Norden, P. R., Kim, D. J., Barry, D. M., Cleaver, O. B. and Davis, G. E. (2016). Cdc42 and k-Ras control endothelial tubulogenesis through apical membrane and cytoskeletal polarization: novel stimulatory roles for GTPase effectors, the small GTPases, Rac2 and Rap1b, and inhibitory influence of Arhgap31 and Rasa1. *PLoS ONE* **11**, e0147758.

Oliver, G. (2004). Lymphatic vasculature development. *Nat. Rev. Immunol.* **4**, 35-45.

Pham, T. H. M., Baluk, P., Xu, Y., Grigorova, I., Bankovich, A. J., Pappu, R., Coughlin, S. R., McDonald, D. M., Schwab, S. R. and Cyster, J. G. (2010). Lymphatic endothelial cell sphingosine kinase activity is required for lymphocyte egress and lymphatic patterning. *J. Exp. Med.* **207**, 17-27.

Schulte-Merker, S., Sabine, A. and Petrova, T. V. (2011). Lymphatic vascular morphogenesis in development, physiology, and disease. *J. Cell Biol.* **193**, 607-618.

Semo, J., Nicenboim, J. and Yaniv, K. (2016). Development of the lymphatic system: new questions and paradigms. *Development* **143**, 924-935.

Serban, D., Leng, J. and Cheresh, D. (2008). H-ras regulates angiogenesis and vascular permeability by activation of distinct downstream effectors. *Circ. Res.* **102**, 1350-1358.

Sosnowski, R. G., Feldman, S. and Feramisco, J. R. (1993). Interference with endogenous ras function inhibits cellular responses to wounding. *J. Cell Biol.* **121**, 113-120.

Srinivasan, R. S., Dillard, M. E., Lagutin, O. V., Lin, F.-J., Tsai, S., Tsai, M.-J., Samokhvalov, I. M. and Oliver, G. (2007). Lineage tracing demonstrates the venous origin of the mammalian lymphatic vasculature. *Genes Dev.* **21**, 2422-2432.

Srinivasan, R. S., Escobedo, N., Yang, Y., Interiano, A., Dillard, M. E., Finkelstein, D., Mukatira, S., Gil, H. J., Nurmi, H., Alitalo, K. et al. (2014). The Prox1–Vegfr3 feedback loop maintains the identity and the number of lymphatic endothelial cell progenitors. *Genes Dev.* **28**, 2175-2187.

Tan, W., Palmby, T. R., Gavard, J., Amornphimoltham, P., Zheng, Y. and Gutkind, J. S. (2008). An essential role for Rac1 in endothelial cell function and vascular development. *FASEB J.* **22**, 1829-1838.

Thomson, B. R., Heinen, S., Jeansson, M., Ghosh, A. K., Fatima, A., Sung, H.-K., Onay, T., Chen, H., Yamaguchi, S., Economides, A. N. et al. (2014). A lymphatic defect causes ocular hypertension and glaucoma in mice. *J. Clin. Invest.* **124**, 4320-4324.

Wang, Y., Nakayama, M., Pitulescu, M. E., Schmidt, T. S., Bochenek, M. L., Sakakibara, A., Adams, S., Davy, A., Deutsch, U., Lüthi, U. et al. (2010). Ephrin-B2 controls VEGF-induced angiogenesis and lymphangiogenesis. *Nature* **465**, 483-486.

Wigle, J. T. and Oliver, G. (1999). Prox1 function is required for the development of the murine lymphatic system. *Cell* **98**, 769-778.

Wilson, C. W., Parker, L. H., Hall, C. J., Smyczek, T., Mak, J., Crow, A., Posthuma, G., De Mazière, A., Sagolla, M., Chalouni, C. et al. (2013). Rasip1 regulates vertebrate vascular endothelial junction stability through Epac1-Rap1 signaling. *Blood* **122**, 3678-3690.

Xu, K., Chong, D. C., Rankin, S. A., Zorn, A. M. and Cleaver, O. (2009). Rasip1 is required for endothelial cell motility, angiogenesis and vessel formation. *Dev. Biol.* **329**, 269-279.

Xu, K., Sacharidou, A., Fu, S., Chong, D. C., Skaug, B., Chen, Z. J., Davis, G. E. and Cleaver, O. (2011). Blood vessel tubulogenesis requires Rasip1 regulation of GTPase signaling. *Dev. Cell.* **20**, 526-539.

Yang, Y. and Oliver, G. (2014). Development of the mammalian lymphatic vasculature. *J. Clin. Invest.* **124**, 888-897.

Yang, Y., García-Verdugo, J. M., Soriano-Navarro, M., Srinivasan, R. S., Scallan, J. P., Singh, M. K., Epstein, J. A. and Oliver, G. (2012). Lymphatic endothelial progenitors bud from the cardinal vein and intersomitic vessels in mammalian embryos. *Blood* **120**, 2340-2348.

Yao, L.-C., Baluk, P., Srinivasan, R. S., Oliver, G. and McDonald, D. M. (2012). Plasticity of button-like junctions in the endothelium of airway lymphatics in development and inflammation. *Am. J. Pathol.* **180**, 2561-2575.

Zheng, W., Nurmi, H., Appak, S., Sabine, A., Bovay, E., Korhonen, E. A., Orsenigo, F., Lohela, M., D'Amico, G., Holopainen, T. et al. (2014). Angiopoietin 2 regulates the transformation and integrity of lymphatic endothelial cell junctions. *Genes Dev.* **28**, 1592-1603.

Supplemental Method

Mouse primary LECs isolation

Mouse primary LECs were isolated from E14.5 embryonic skin. Tissue digestion was performed as described previously (Stanczuk et al, 2015). Briefly, embryonic skin was cut into smaller pieces for digestion using a mixture of 5 mg/ml Collagenase IV (Life Technologies) and 0.2 mg/ml DNase (Roche) in PBS with 5% fetal bovine serum (FBS) at 37°C under constant rotation for 45min. Digests were quenched by adding 2 mM EDTA and filtered through a 70-µm nylon filter (BD Biosciences). LECs were purified by using a MiniMACS separator and Starting Kit (Miltenyi Biotec). Briefly, digested cell solutions were centrifuged and resuspended in PBS with 0.5%BSA and 2 mM EDTA at approx 10^8 cells/ml. Macrophages and leukocytes were removed by adding rat anti-F480 and CD45 (BD Biosciences) antibodies and Goat anti-Rat IgG microbeads and purified on MACS MS column according to manufacturers' instructions. Flow through was collected and incubated with microbeads conjugated goat anti-Lyve1 antibodies. Lyve1 positive LECs were purified on MACS MS columns and eluted according to the manufacturers protocol.

Supplemental Reference

Stanczuk L., Martinez-Corral I., Ulvmar MH., Zhang Y., Laviña B., Fruttiger M., Adams RH., Saur D., Betsholtz C., Ortega S., et al. (2015). cKit Lineage Hemogenic Endothelium-Derived Cells Contribute to Mesenteric Lymphatic Vessels. *Cell Rep*. **10**,1708–1721.

Development • Supplementary information

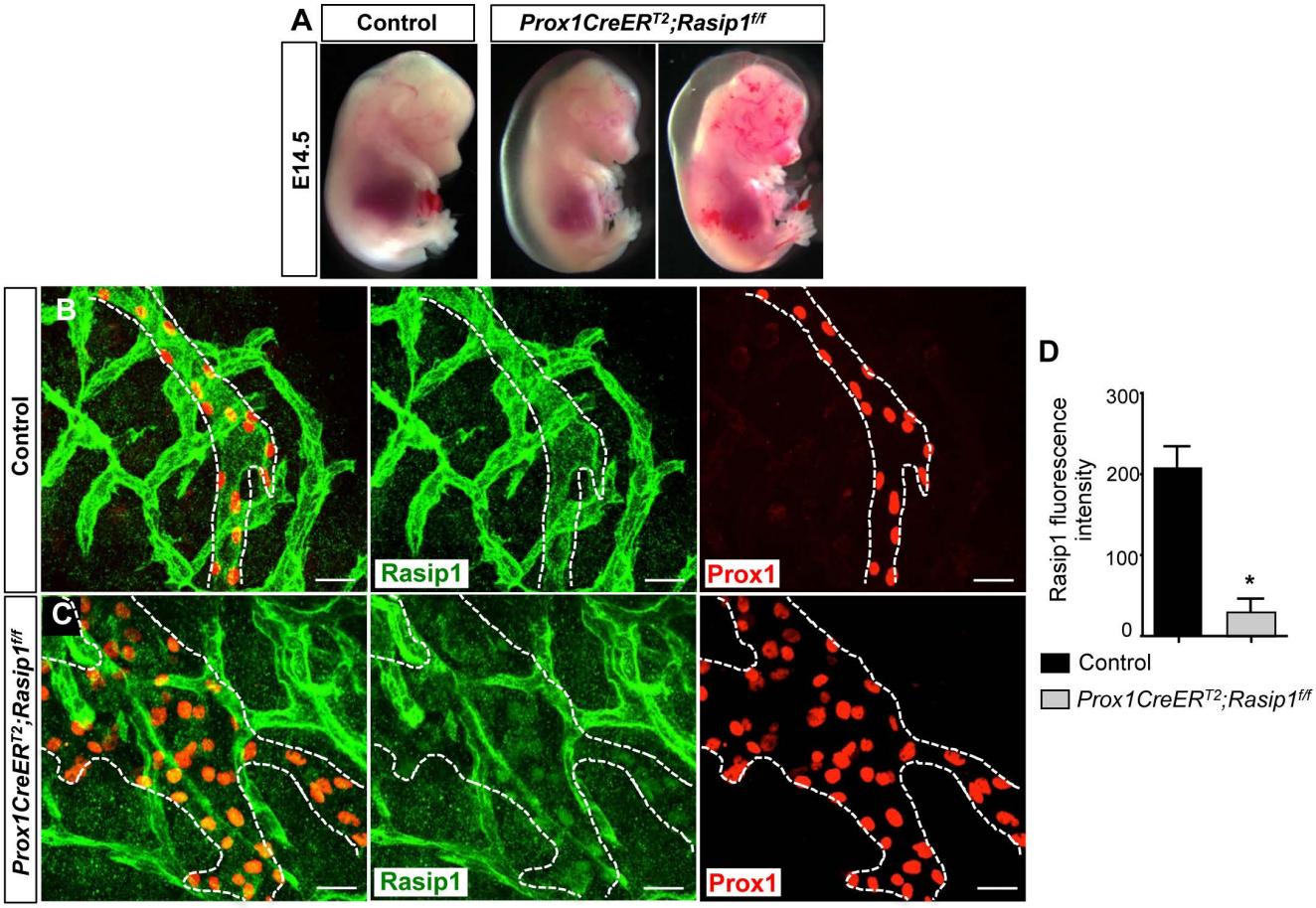

Fig. S1. Dermal lymphatics become enlarged and dilated in E14.5 *Prox1CreER^{T2};Rasip1$^{f/f}$* embryos

A) Representative images of E14.5 control and *Prox1CreER^{T2};Rasip1$^{f/f}$* embryos. *Prox1CreER^{T2};Rasip1$^{f/f}$* embryos exhibit severe edema (*n*=8) and some have also blood-filled lymphatics (*n*=4). **B, C)** Whole mount immunostaining of E14.5 dermal lymphatics of control (*n*=3) and *Prox1CreER^{T2};Rasip1$^{f/f}$* (*n*=3) embryos. Scale bar: 25 um. **D**) Quantification of Rasip1 fluorescence intensity in both genotypes. Data are derived from 6 fields per genotype. Results are expressed as mean ± SEM. **p*<0.05 vs control. Student T test.

Development • Supplementary information

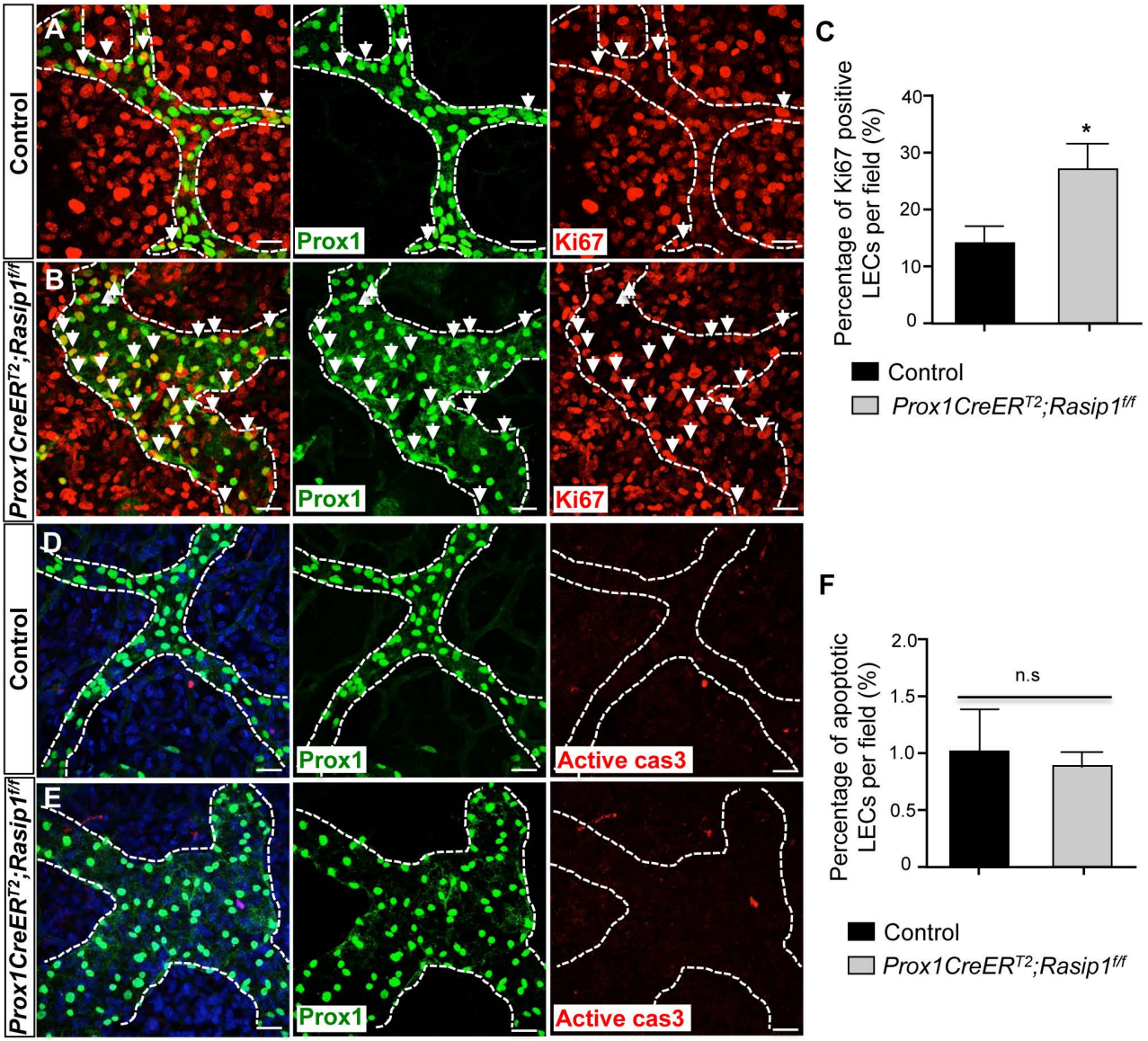

Fig. S2. Increased proliferation rate in skin lymphatics of E14.5 *Prox1CreER^{T2};Rasip1$^{f/f}$* embryos

A, B) Whole mount immunostaining of E14.5 skin lymphatics in control (*n*=3) and *Prox1CreER^{T2};Rasip1$^{f/f}$* embryos (*n*=3) using antibodies against Ki67 and Prox1. Arrows indicates Ki67 positive LECs. An obvious increase in the number of proliferating LECs is seen in the mutant embryos. Scale bar: 25 um. **C**) Quantification of the percentage of Ki67 positive LECs in both genotypes. Data are derived from 5 randomly selected fields per genotype. Results are expressed as mean ± SEM. **p*<0.05 vs control. Student T test. **D, E)** Whole mount staining of E14.5 skin lymphatics in control (*n*=4) and *Prox1CreER^{T2};Rasip1$^{f/f}$* embryos (*n*=3) with antibodies against active caspase-3 and Prox1. No obvious differences in cell death were observed. Scale bar: 25 um. **F)** Quantification of the percentage of active caspase-3 positive LECs in both genotypes. Data are derived from 5 randomly selected fields per genotype. Results are expressed as mean ± SEM. **p*<0.05 vs control. Student T test. TM was induced at E9.5 and E10.5.

Development • Supplementary information

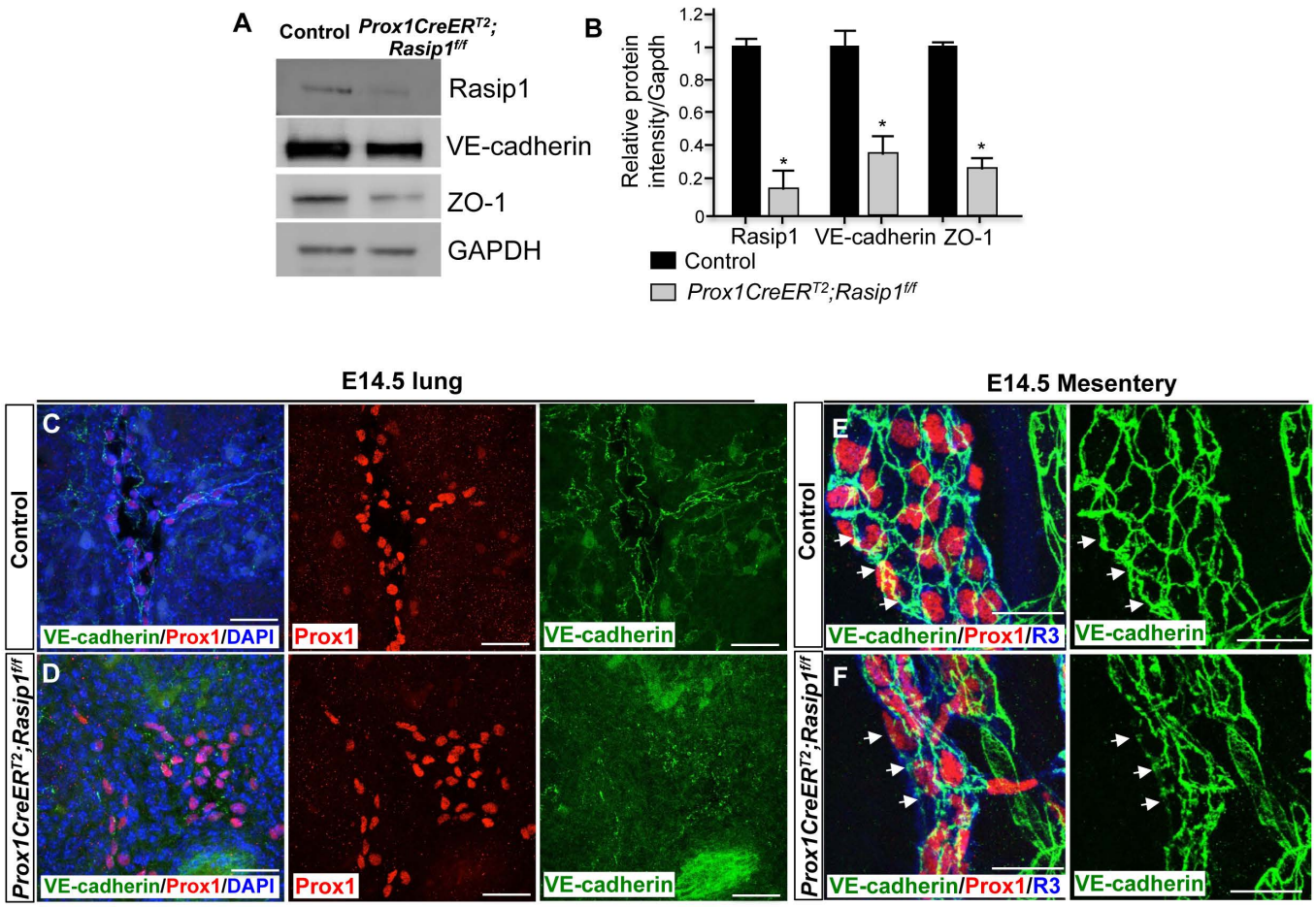

Fig. S3. Endothelial cell junctions are disorganized and expression of VE-cadherin is reduced in E14.5 *Prox1CreER^{T2};Rasip1$^{f/f}$* embryos

A) Western blot analysis of LECs isolated from E14.5 control (n=4) and *Prox1CreER^{T2};Rasip1$^{f/f}$* (n=4) skin lymphatics using antibodies against Rasip1, VE-cadherin, ZO-1 and GAPDH. As shown there, Rasip1 deletion was highly efficient and as seen *in vivo*, the levels of VE-cadherin and ZO-1 are reduced. **B)** Quantification of Rasip1, VE-cadherin and ZO-1 levels in isolated LECs of control and *Prox1CreER^{T2};Rasip1$^{f/f}$* embryos. Results are expressed as mean ± SEM of 3 triplicate experiments. **p*<0.05 vs control. Student T test. **C, D)** Immunostaining of thick sections (20 um) of lung lymphatics in E14.5 control (*n*=3) and *Prox1CreER^{T2};Rasip1$^{f/f}$* (*n*=3) embryos with antibodies against VE-cadherin and Prox1 and counterstained with DAPI. VE-cadherin-expressing junctions appeared disorganized in the mutant embryos. Scale bar: 50 um. **E, F)** Whole mount staining of E14.5 control (*n*=3) and *Prox1CreER^{T2};Rasip1$^{f/f}$* (*n*=3) mesentery lymphatics with antibodies against VE-cadherin, VEGFR3 and Prox1. Normal cell junctions are seen in control embryos (arrows); however, these are disorganized and diffuse in mutant embryos (arrows). Scale bar: 25 um.

Development • Supplementary information

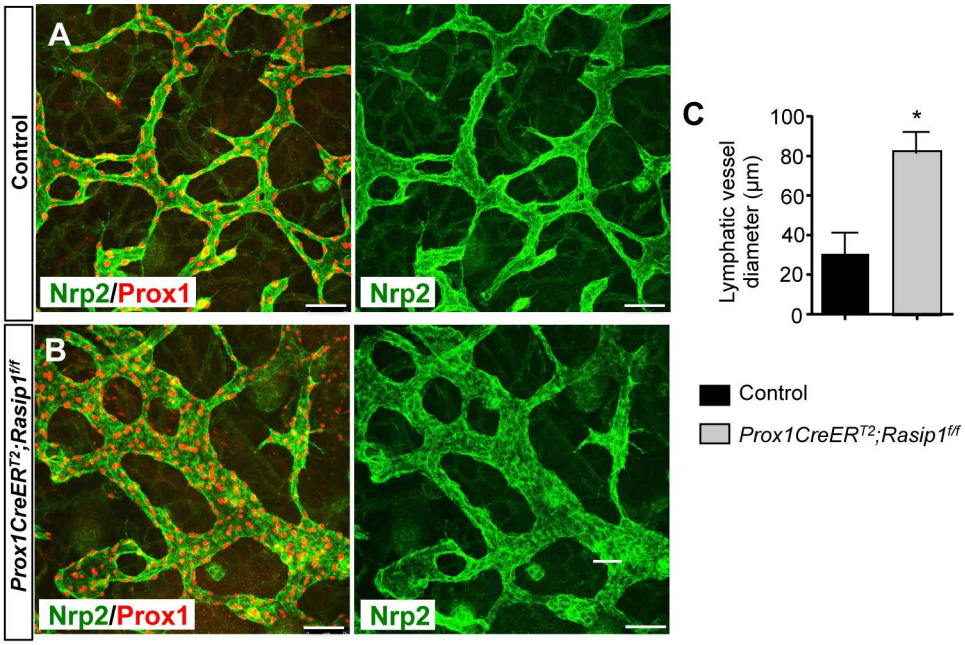

Fig. S4. Enlarged dermal lymphatic vessels in E14.5 *Prox1CreER^{T2};Rasip1$^{f/f}$* embryos

A, B) Whole mount staining of dermal lymphatics in E14.5 control (A) (*n*=3) and *Prox1CreER^{T2};Rasip1$^{f/f}$* (B) (*n*=3) embryos with antibodies against Nrp2 and Prox1. Scale bar: 75 um. **C)** Quantification of lumen diameters in dermal lymphatics of control and *Prox1CreER^{T2};Rasip1$^{f/f}$* embryos. Data are derived from 6 randomly selected fields per genotype. Results are expressed as mean ± SEM. **p*<0.05 vs control. Student T test. TM was induced at E9.5 and E10.5.

Development • Supplementary information

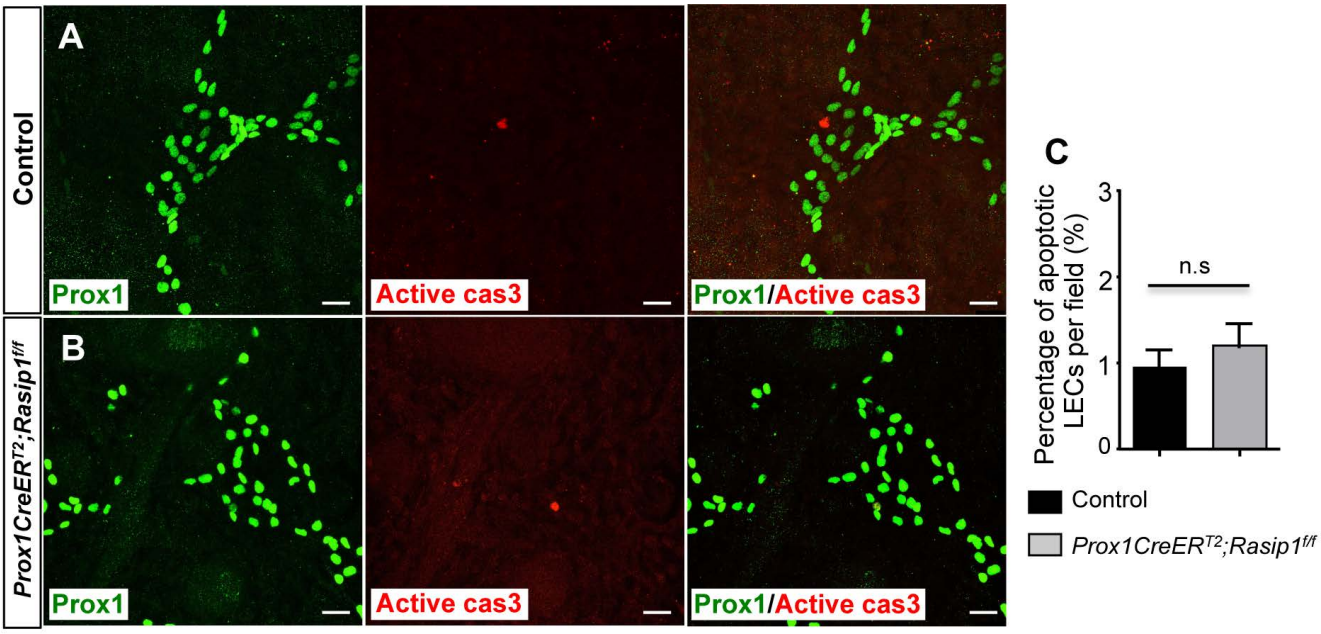

Fig. S5. No difference in LEC apoptosis in E16.0 *Prox1CreER^{T2};Rasip1$^{f/f}$* embryos

A, B) Whole mount staining of E16.0 control (*n*=3) and *Prox1CreER^{T2};Rasip1$^{f/f}$* (*n*=3) skin lymphatic vessels with antibodies against Prox1 and active caspase-3. Scale bar: 25 um. **C)** Quantification of percentage of active caspase-3 positive LECs in skin samples of E16.0 control and *Prox1CreER^{T2};Rasip1$^{f/f}$* embryos. Data are derived from 6 randomly selected fields per genotype. Results are expressed as mean ± SEM. Student T test. TM was induced at E9.5 and E10.5.

Development • Supplementary information

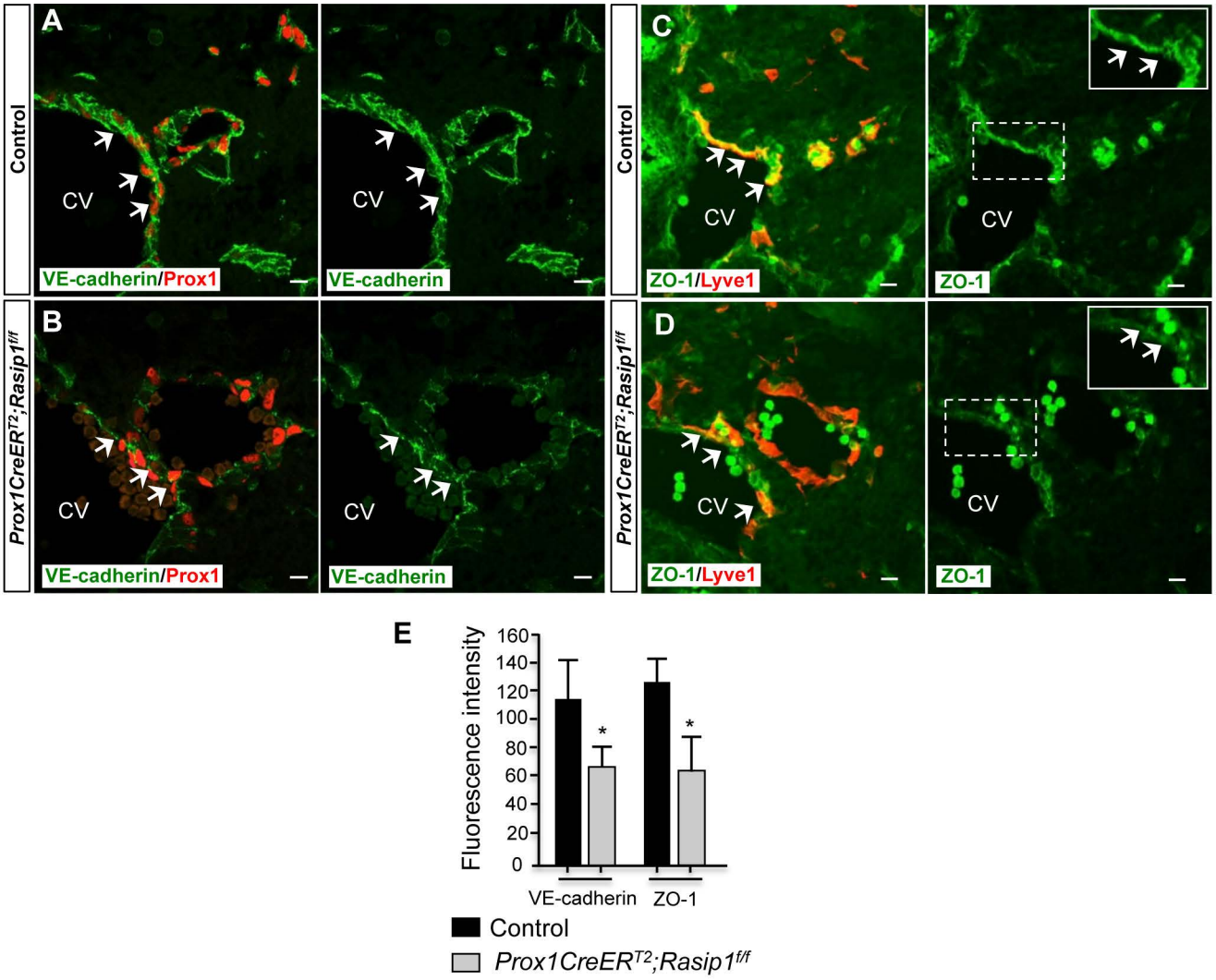

Fig. S6. LEC cell junction levels are reduced in E11.5 *Prox1CreER^{T2};Rasip1$^{f/f}$* embryos
A, B) Immunostaining of E11.5 transverse sections of control (*n*=3) and *Prox1CreER^{T2};Rasip1$^{f/f}$* embryos (*n*=3) at the level of the anterior cardinal vein (CV) with antibodies against VE-cadherin and Prox1. Arrows indicate Prox1-expressing LEC progenitors. LEC progenitors are seen also inside the CV of conditional mutant embryos and also budding off into the surrounding mesenchyme. However, the levels of VE-cadherin are strongly downregulated in those mutant LECs. **C, D)** Additional sections of E11.5 control (*n*=3) and *Prox1CreER^{T2};Rasip1$^{f/f}$* (*n*=3) embryos were immunostained against ZO-1 and Lyve1. Arrows indicate ZO-1 expressing LEC progenitors. Similar to VE-cadherin, the levels of ZO-1 were severely reduced in the mutant embryos. Upper right panels in green channels show higher magnification of selected regions. TM was induced at E9.5 and E10.5. Scale bars are all 10 um. **E)** Quantification of relative fluorescence intensity for VE-cadherin and ZO-1 staining at E11.5 in control and *Prox1CreER^{T2};Rasip1$^{f/f}$* embryos. Data are derived from 5 randomly selected fields per genotype per stage. Results are expressed as mean ± SEM. *p<0.05 vs control. Student T test.

Development • Supplementary information

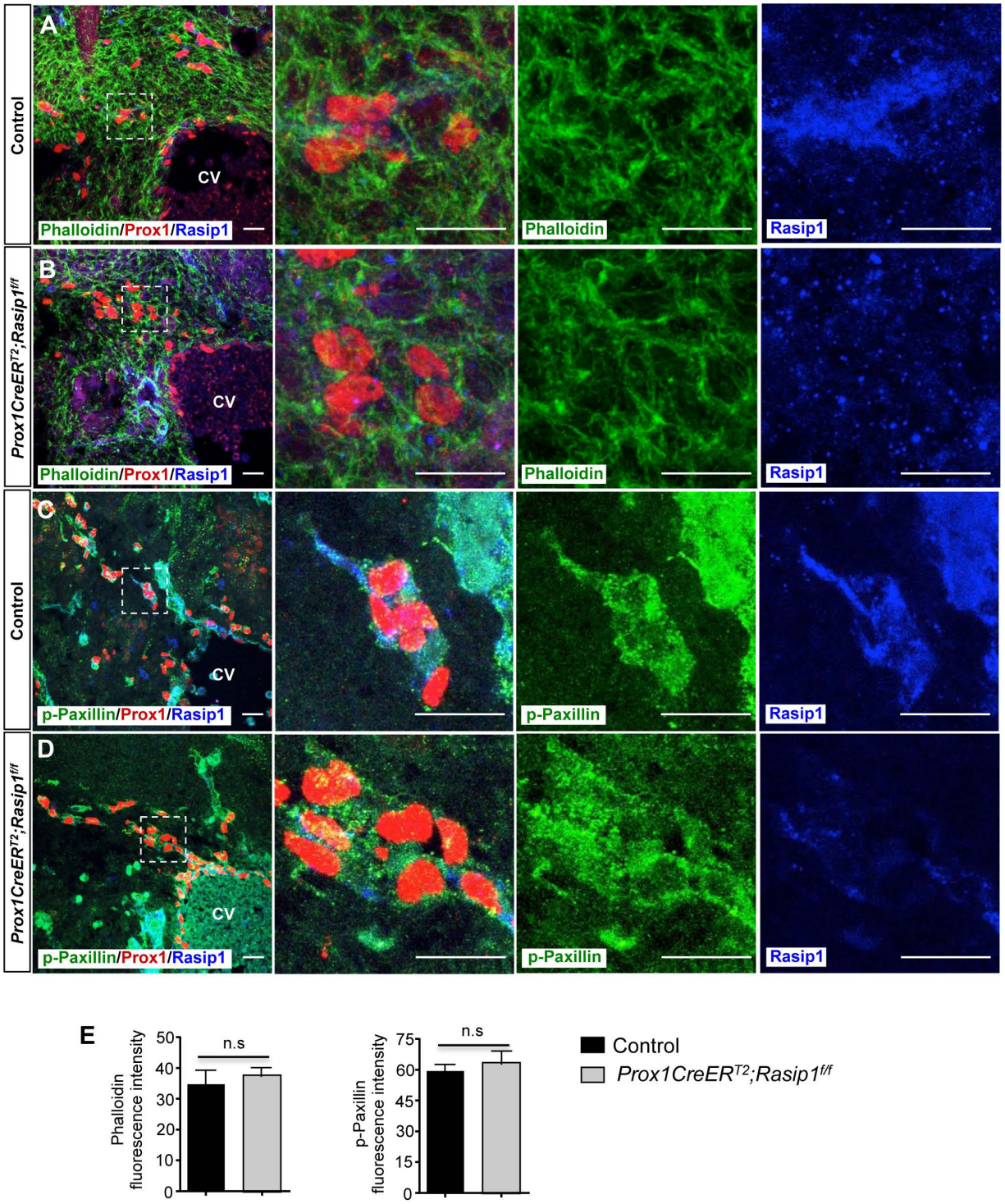

Fig. S7. No difference in cytoskeleton organization or LEC-ECM interactions in E11.5 *Prox1CreER^{T2};Rasip1$^{f/f}$* embryos

A-D) Immunostaining of E11.5 transverse sections of control (*n*=3) and *Prox1CreER^{T2};Rasip1$^{f/f}$* embryos (*n*=3) at the level of the anterior cardinal vein (CV) with 488-conjugated Phalloidin and antibodies against Prox1 and Rasip1 (A, B) or antibodies against p-Paxillin, Prox1 and Rasip1 (C, D). Right panels show higher magnification of selected regions. Rasip1 staining suggests sufficient deletion in LECs in *Prox1CreER^{T2};Rasip1$^{f/f}$* embryos. Scale bars are all 10 um. **E)** Quantification of fluorescence intensity for Phalloindin labeling and p-Paxillin staining in LECs in control and *Prox1CreER^{T2};Rasip1$^{f/f}$* embryos. Data are derived from 6 randomly selected fields per genotype per stage. Results are expressed as mean ± SEM. Student T test. TM was induced at E9.5 and E10.5.

Development • Supplementary information

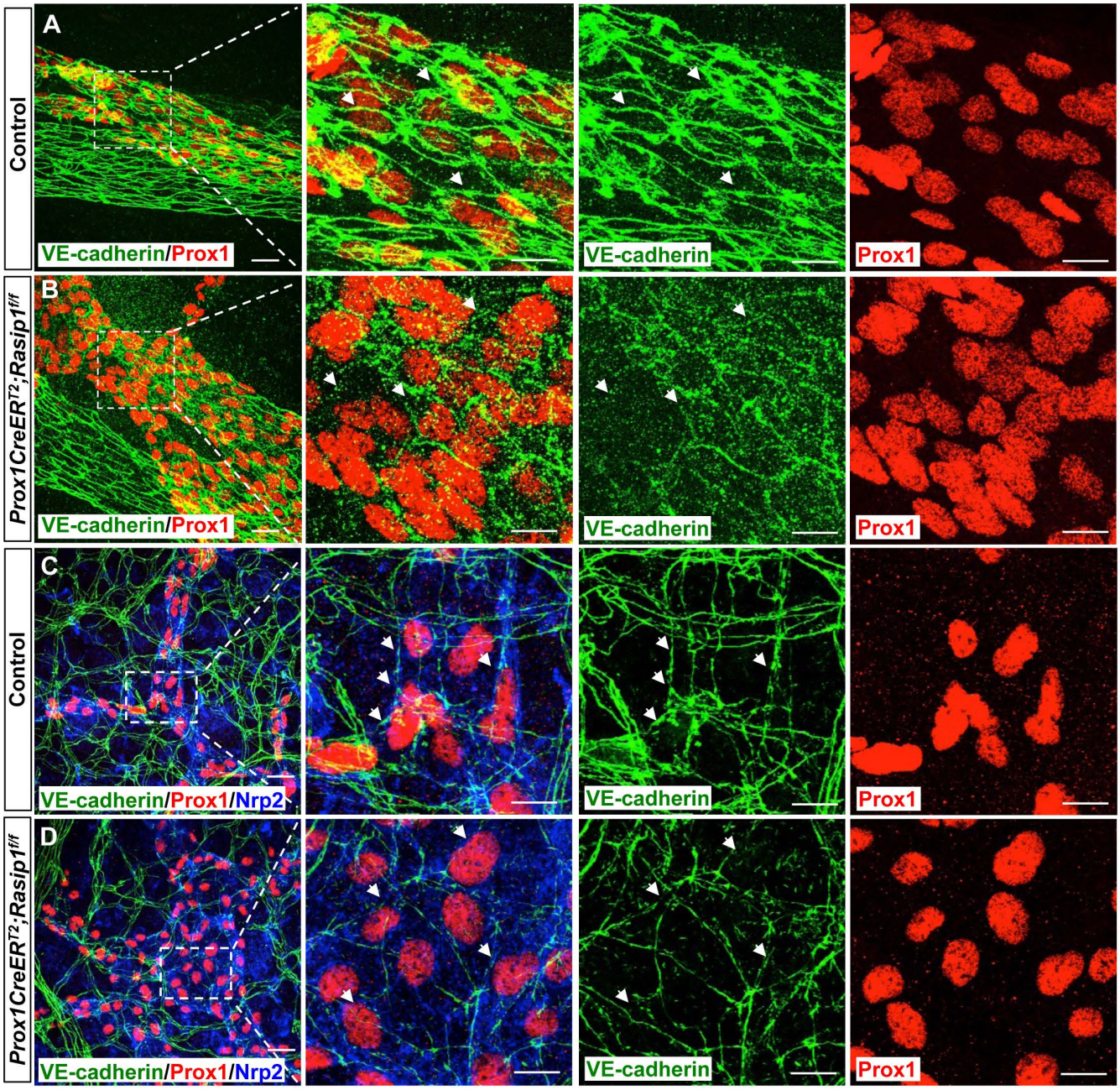

Fig. S8. Disorganized cell junctions in E17.5 *Prox1CreER^{T2};Rasip1$^{f/f}$* lymphatic vessels
A, B) Whole mount staining of mesentery lymphatics in E17.5 control (*n*=3) and *Prox1CreER^{T2};Rasip1$^{f/f}$* (*n*=3) embryos with antibodies against VE-cadherin and Prox1. The right panels show a higher magnification of the selected regions indicated in the left panels. White arrow indicates VE-cadherin junctions. Scale bar: 25 um. **C, D)** Whole mount staining of skin lymphatics in E17.5 control (*n*=3) and *Prox1CreER^{T2};Rasip1$^{f/f}$* (*n*=3) embryos with antibodies against VE-cadherin, Nrp2 and Prox1. The right panels show a higher magnification of the selected regions indicated in the left panels. White arrows indicate VE-cadherin junctions. TM was induced at E14.5. Scale bar: 25 um.

Development • Supplementary information

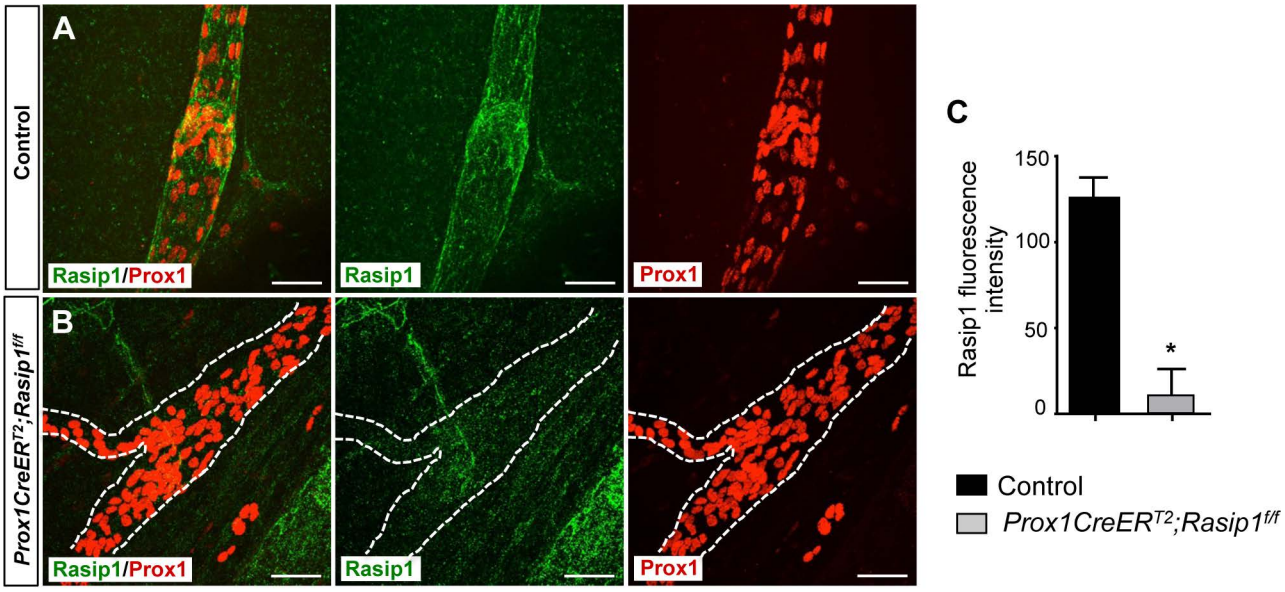

Fig. S9. *Rasip1* deletion efficiency in P6 *Prox1CreER^{T2};Rasip1$^{f/f}$* collecting lymphatic vessels

A, B) Whole mount staining of P6 mesentery lymphatics in control (*n*=5) and *Prox1CreER^{T2};Rasip1$^{f/f}$* (*n*=4) embryos with antibodies against Rasip1 and Prox1. Dashed line outline the collecting lymphatic vessel. Scale bar: 50 um. **C)** Quantification of fluorescence intensity for Rasip1 staining in control and *Prox1CreER^{T2};Rasip1$^{f/f}$* embryos. Data are derived from 6 randomly selected fields per genotype per stage. Results are expressed as mean ± SEM. **p*<0.05 vs control. Student T test. TM was induced from P0 to P4.

Development • Supplementary information

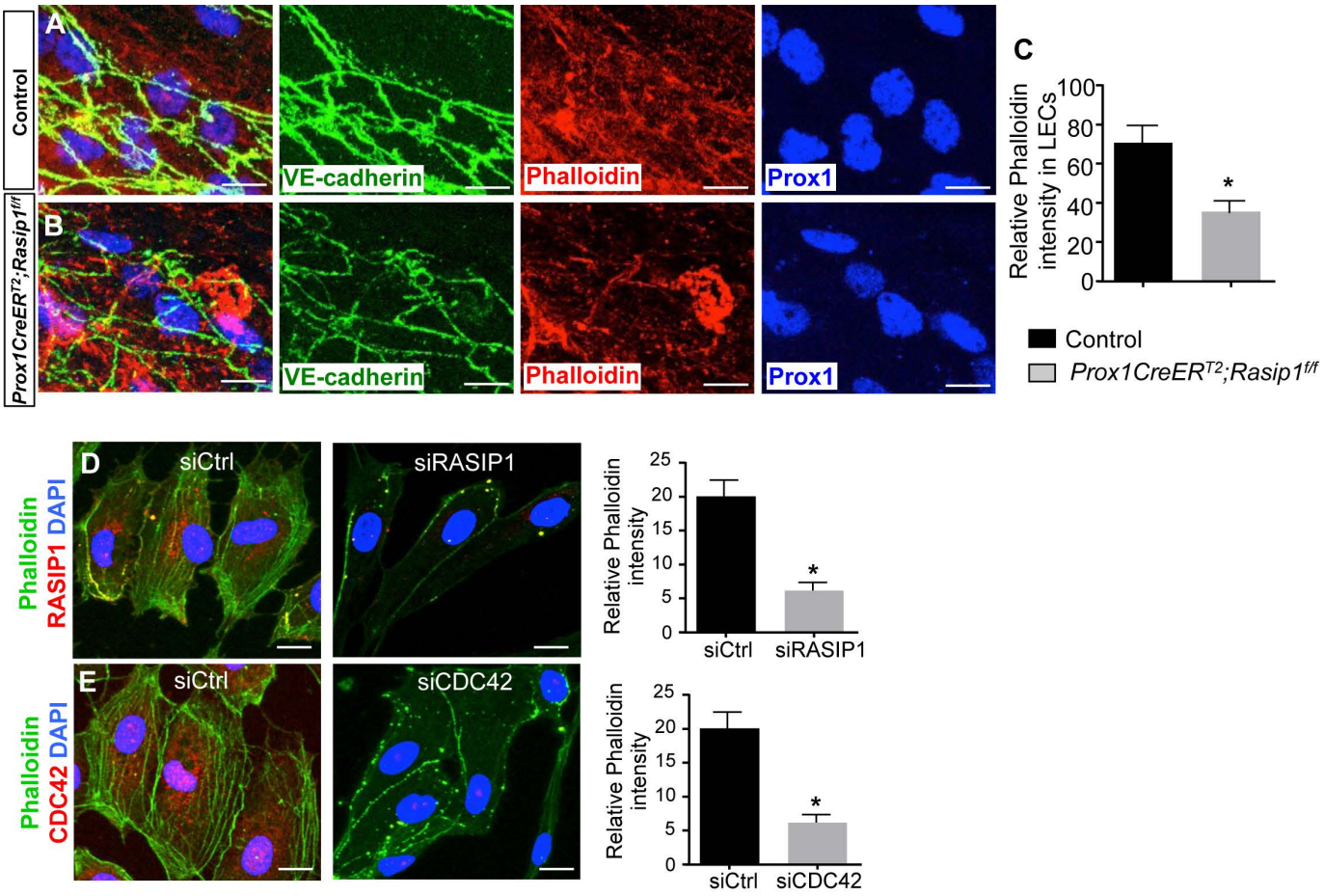

Fig. S10. Abnormal cytoskeleton organization in Rasip1 deficient LECs *in vivo* and *in vitro*
A, B) Whole mount staining of E14.5 mesentery lymphatics in control (*n*=3) and *Prox1CreER^{T2};Rasip1$^{f/f}$* (*n*=3) embryos with antibodies against VE-cadherin, Prox1 and Cy3-conjugated Phalloidin. TM was induced at E9.5 and E10.5. **C)** Quantification of Phalloidin intensity in mesentery lymphatics of control and *Prox1CreER^{T2};Rasip1$^{f/f}$* embryos. Data are derived from 5 randomly selected fields per genotype. Results are expressed as mean ± SEM. **p*<0.05 vs control. Student T test. **D, E)** Immunostaining of control, RASIP1 siRNA (siRASIP1) or CDC42 siRNA (siCDC42) treated human dermal LECs with antibodies against RASIP1, CDC42 and 488-conjugated Phalloidin. Experiments were repeated three times. Scale bars are all 10 um. Quantifications of Phalloidin intensity are shown at right panel. Data are derived from 5 randomly selected fields per genotype. Results are expressed as mean ± SEM. **p*<0.05 vs control. Student T test.

Development • Supplementary information

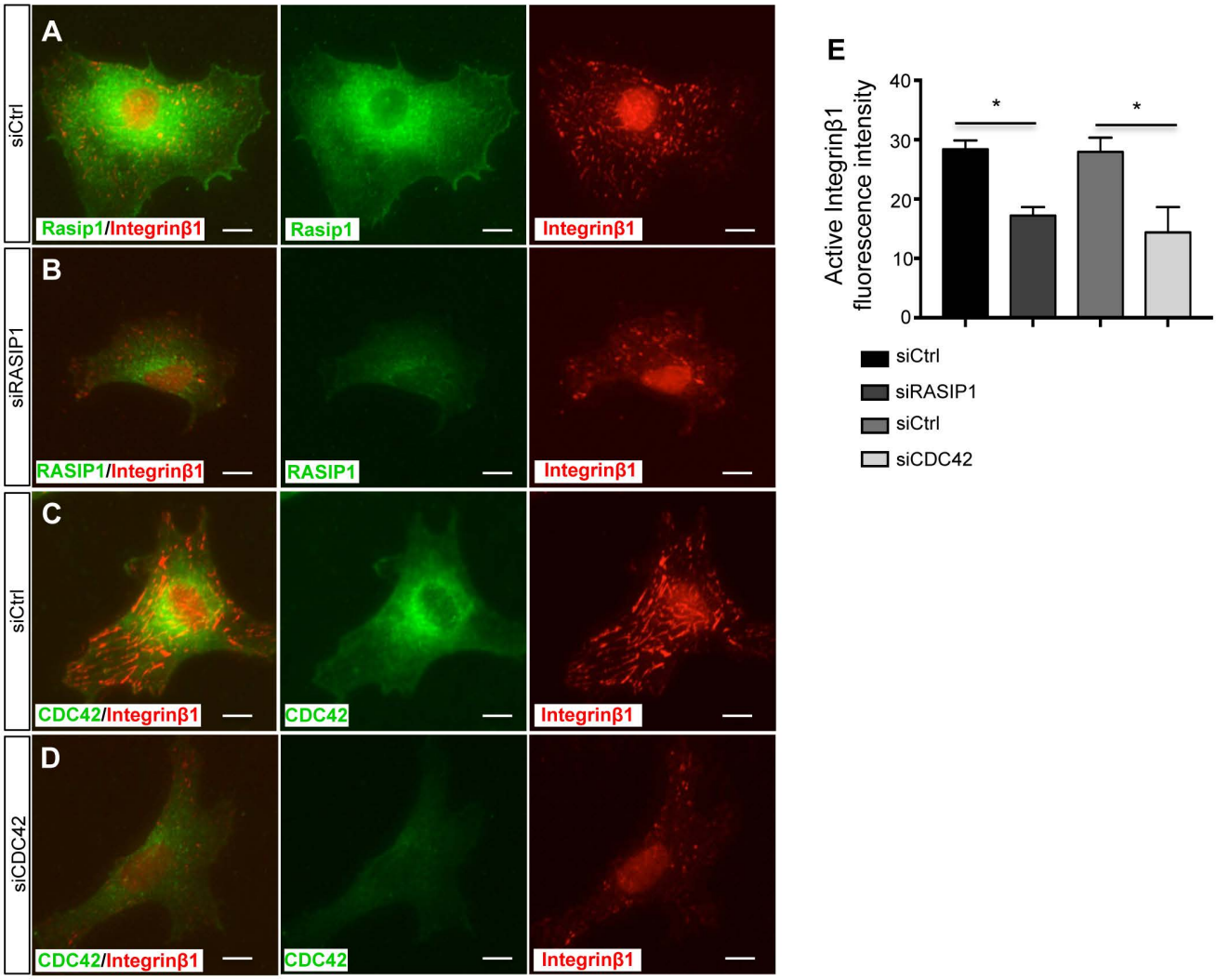

Fig. S11. Reduced mature focal adhesion activities in siRASIP1 or siCDC42 treated LECs. A-D) Immunostaining of siCtrl, siRASIP1 or siCDC42-treated LECs with antibodies against RASIP1 and active Integrinβ1 (A, B) or CDC42 and active Integrinβ1 (C, D). The levels of active Integrinβ1 are drastically reduced in the siRASIP1 or siCDC42-treated LECs. Scale bar, 10 um. **E)** Quantifications of active Integrinβ1 levels in siCtrl, siRASIP1 and siCDC42-treated cells. Data are derived from 6 randomly selected fields per group. Results are expressed as mean ± SEM. *p<0.05 vs siCtrl. Student T test.

Development • Supplementary information

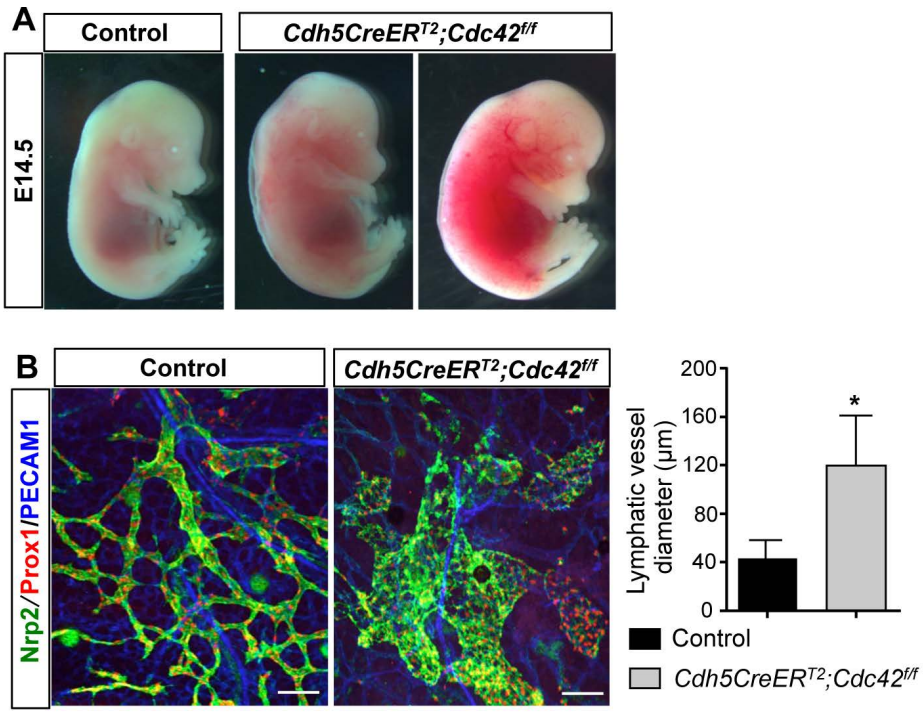

Fig. S12. Dermal lymphatics are enlarged and dilated in E14.5 *Cdh5CreER^{T2};Cdc42$^{f/f}$* embryos

A) Representative bright field images of E14.5 control (*n*=5) and *Cdh5CreER^{T2};Cdc42$^{f/f}$* (*n*=3) embryos. **B)** Whole mount staining of E14.5 dermal lymphatics of control (*n*=3) and *Cdh5CreER^{T2}; Cdc42$^{f/f}$* (*n*=3) embryos. Lymphatics are abnormally dilated in the mutant embryos. Scale bar: 100 um. Quantification of lymphatic vessel diameters in both genotypes is shown in the right panel. Data are derived from 6 randomly selected fields per genotype. Results are expressed as mean ± SEM. **p*<0.05 vs control. Student T test.

Development • Supplementary information

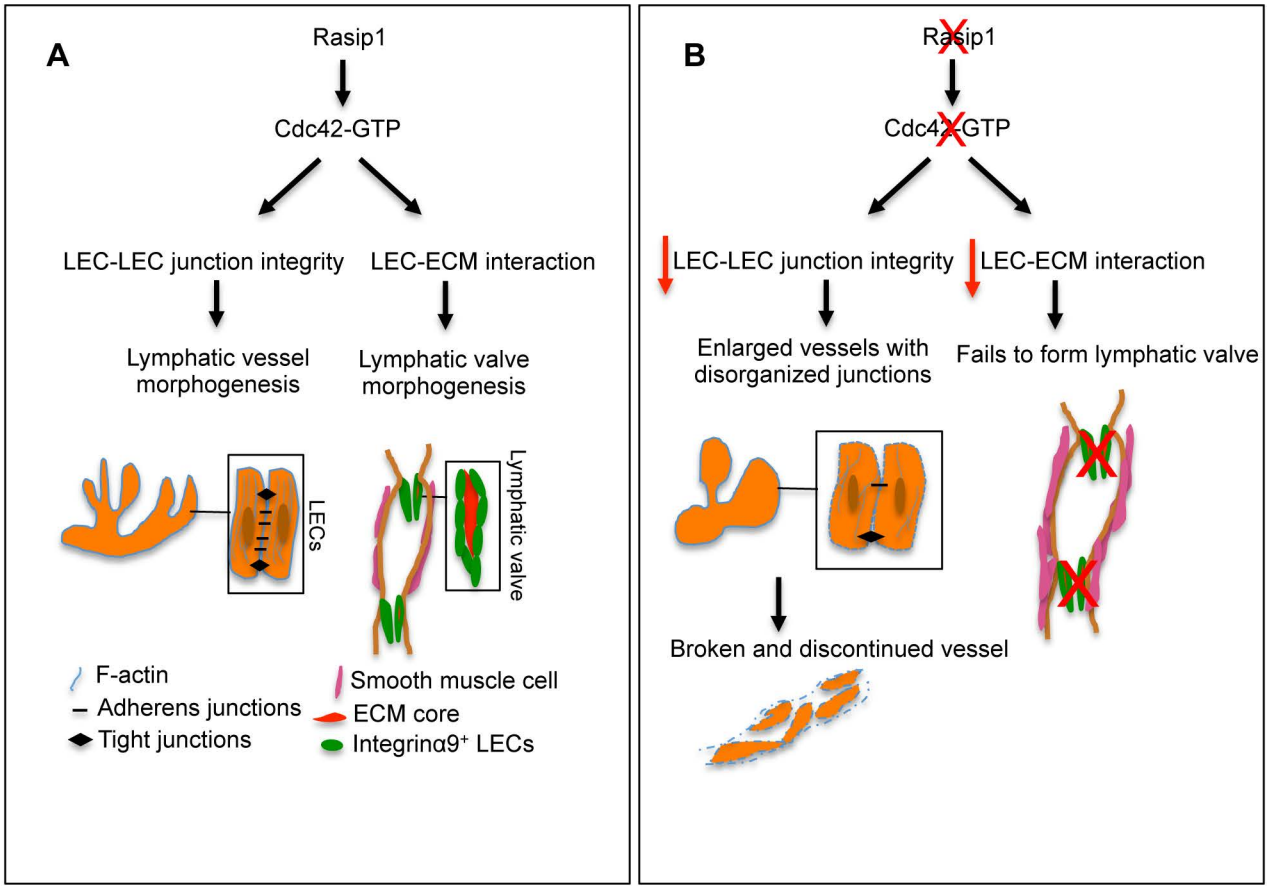

Fig. S13. *Rasip1* regulates LEC cell junction integrity and lymphatic valve formation by regulating Cdc42 activity

A) In control embryos *Rasip1* regulation of Cdc42 activity in LECs is required for cytoskeleton organization which in turn promotes lymphatic endothelial junctions' integrity to ensure lumen maintenance and proper lymphatic vessel morphogenesis. During lymphatic valve development, *Rasip1* regulates Cdc42 activity in valve-forming cells to modulate LEC interactions with the surrounding ECM. **B)** Loss of *Rasip1* abolishes Cdc42 activity, thus LECs show disorganized cytoskeleton localization which impairs proper LEC junctions' integrity. Therefore, developing lymphatic vessels get fragmented and lose their lumen. During lymphatic valve development, loss of *Rasip1* leads to defective LEC-ECM interactions in LECs resulting in defective lymphatic valve formation.

Development • Supplementary information